Nonlinear Analysis: Hybrid Systems 25 (2017) 263–282

Contents lists available at ScienceDirect

Nonlinear Analysis: Hybrid Systems

journal homepage: www.elsevier.com/locate/nahs

Hybrid optimal control of an electric vehicle with a dual-planetary transmission

Ali Pakniyat *, Peter E. Caines

Centre for Intelligent Machines (CIM) and the Department of Electrical and Computer Engineering, McGill University, Montreal, Canada

ARTICLE INFO

Article history:
Available online 24 September 2016

Keywords:
Optimal control
Hybrid systems
Minimum Principle
Electric vehicle
Gear selection

ABSTRACT

A hybrid systems framework is presented for the analysis and optimal control of an electric vehicle equipped with a seamless dual stage planetary transmission. A feature of special interest is that, due to the perpetual connectedness of the motor to the wheels via the seamless transmission, the mechanical degree of freedom changes during the transition period. These circumstances where autonomous and controlled state jumps at the switching instants are accompanied by changes in the dimension of the state space are reflected in the definition of hybrid systems and the corresponding statement of the Hybrid Minimum Principle (HMP). Furthermore, the state-dependent motor torque constraints which impose mixed input-state constraints are converted to state-independent input constraints via a change of variables and the introduction of auxiliary discrete states. Optimal control problems for the minimization of acceleration duration and the minimization of energy consumption for the acceleration task are formulated within the presented framework and simulation results are presented for the optimal control inputs and the optimal gear changing instants for reaching the speed of 100 km/hr from the stationary initial condition. A phenomenon of note that appears in the dynamical evolution of the vehicle is the presence of power regeneration as a part of the acceleration task for the minimization of the energy consumption.

1. Introduction

The Minimum Principle (MP), also called the Maximum Principle in the pioneering work of Pontryagin et al. [1], is a milestone of systems and control theory that led to the emergence of optimal control as a distinct field of research. This principle states that any optimal control along with the optimal state trajectory must solve a two-point boundary value problem in the form of an extended Hamiltonian canonical system, as well as an extremization condition of the Hamiltonian function. Whether the extreme value is maximum or minimum depends on the sign convention used for the Hamiltonian definition. The generalization of the Minimum Principle for hybrid systems, i.e. control systems with both continuous and discrete states and dynamics, results in the Hybrid Minimum Principle (HMP) (see e.g. [2–14]). The HMP gives necessary conditions for the optimality of the trajectory and the control inputs of a given hybrid system with fixed initial conditions and a sequence of autonomous and controlled switchings. These conditions are expressed in terms of the minimization of the distinct Hamiltonians indexed by the discrete state sequence of the hybrid trajectory. A feature of special interest is the boundary conditions on the adjoint processes and the Hamiltonian functions at autonomous and controlled

* Corresponding author.
E-mail addresses: pakniyat@cim.mcgill.ca (A. Pakniyat), peterc@cim.mcgill.ca (P.E. Caines).

http://dx.doi.org/10.1016/j.nahs.2016.08.004
1751-570X/

switching times and states; these boundary conditions may be viewed as a generalization of the optimal control case of the Weierstrass–Erdmann conditions of the calculus of variations [15].

The goal of this paper is to present a hybrid systems formulation of an electric vehicle equipped with a dual-stage planetary transmission presented in [16,17] and employ hybrid optimal control theory to find the optimal inputs for the gear changing problem for electric vehicles. The seamless dual brake transmission under study is designed particularly for electric vehicle in order to reduce the size of the electric motor and provide an appropriate balance between efficiency and dynamic performance (see [16–18] and the references therein for more discussion about industrial motivations for the particular design). Due to the special structure of the transmission under study, the mechanical degree of freedom and therefore, the dimension of the (continuous) state space of the system depend on the status of the transmission, i.e. whether a gear number is fixed or the system is undergoing a transition between the two gears. Therefore, the modelling of the powertrain requires the consideration of autonomous and controlled state jumps accompanied by changes in the dimension of the state space.

These characteristics are reflected in the definition of hybrid systems in Section 2 and Appendix A, where a general class of nonlinear systems on Euclidean spaces are considered whose dimensions depend upon their corresponding discrete states, and where autonomous and controlled switchings and jumps between different state spaces are allowed at the switching states and times. A general class of optimal control problems associated with the presented hybrid systems framework is introduced with a large range of running, terminal and switching costs. Other hybrid optimal control frameworks presented in the rich literature on hybrid optimal control theory (see e.g. [2–10,19–26]) may be obtained via variations and specializations of the framework presented here. In Section 3, the statement of the Hybrid Minimum Principle for the class of hybrid optimal control problems under study is presented. Distinctive aspects of the HMP presented here in comparison with other versions of the HMP are the presence of state dependent switching costs, the possibility of state space dimension change, and the existence of low dimensional switching manifolds.

In Section 4 we extend the formulation presented in [18] for the dynamics and energy consumption of gear-equipped electric vehicles by the inclusion of the transmission dynamics, considering the model of a seamless dual brake transmission reported in [16,17]. After presenting the Kinematic relations in the driveline, the dynamics of the powertrain is derived from the Principle of Virtual Work and the generalized Euler–Lagrange equation. In order to avoid state-dependent input constraints imposed by the maximum torque and maximum power constraints of the electric motor (see also Fig. 2) the state-dependent input constraints are converted to state-independent constraints via a change of variables and the introduction of auxiliary discrete states. The corresponding hybrid systems formulation which is an extension of [27] is presented in Section 5.

In Section 6 the hybrid optimal control problem is considered to be the minimization of the time required for reaching the speed of 100 km/h from the stationary state (see also [27]). In Section 7 a similar manoeuvre is considered but, in contrast, the minimization of the energy consumption is studied for performing the same task on a longer time horizon. The Hybrid Minimum Principle is employed to find the optimal control inputs and optimal switching instants for both problems and simulation results are presented. A phenomenon of note that appears in the dynamical evolution of the vehicle in the energy optimal mode is the presence of power regeneration as a part of the optimal control for the acceleration task.

2. Hybrid optimal control problems

Informally speaking, a hybrid system is a control system whose state is composed of both discrete state components $q \in Q$, and continuous state components $x \in \mathbb{R}^{n_q}$, and whose input is composed of both discrete input components $\sigma \in \Sigma$, and continuous input components $u \in U_q$, for which the evolution of the continuous state [component] is governed by a set of controlled vector fields $f_q \in F$, in the form of

$$\dot{x}_{q_i}(t) = f_{q_i}\left(x_{q_i}(t), u_{q_i}(t)\right), \quad \text{a.e. } t \in [t_i, t_{i+1}), \tag{1}$$

subject to initial and boundary conditions

$$x_{q_0}(t_0) = x_0, \tag{2}$$

$$x_{q_j}(t_j) = \xi_{\sigma_{q_{j-1}q_j}}\left(x_{q_{j-1}}(t_j-)\right) \equiv \xi_{\sigma_{q_{j-1}q_j}}\left(\lim_{t\uparrow t_j} x_{q_{j-1}}(t)\right), \tag{3}$$

where $0 \leq i \leq L$, $1 \leq j \leq L$, $t_{L+1} = t_f < \infty$, and at the switching instants t_j, the updates in the discrete state [component] are governed by a finite automata A and its corresponding transition map Γ. Switchings are referred to as autonomous switchings if they are constrained upon transversal arrival of the continuous state trajectory on a switching manifold described locally by

$$m_{q,r} = \left\{x \in \mathbb{R}^{n_q} : m^1_{q,r}(x) = 0 \wedge \cdots \wedge m^k_{q,r}(x) = 0\right\}, \tag{4}$$

where $m_{q,r} \in \mathcal{M}$, $q, r \in Q$, $r \in A(q, \sigma)$, $\sigma \in \Sigma$, and $1 \leq k \leq n_q$. Controlled switchings, in contrast, are direct results of the (hybrid) input command.

The overall hybrid dynamics can be described in a hybrid automata diagram as illustrated in Fig. 3 for an electric vehicle equipped with a dual planetary transmission studied in this paper.

The objective of the associated hybrid optimal control problem is to find hybrid input(s) I_L to infimize a hybrid performance measure in the form of

$$J\left(t_0, t_f, h_0, L; I_L\right) := \sum_{i=0}^{L} \int_{t_i}^{t_{i+1}} l_{q_i}\left(x_{q_i}(s), u(s)\right) ds + \sum_{j=1}^{L} c_{\sigma_{q_{j-1}q_j}}\left(t_j, x_{q_{j-1}}\left(t_j-\right)\right) + g\left(x_{q_L}\left(t_f\right)\right). \tag{5}$$

A formal definition together with the underlying assumptions is presented in Appendix A.

3. Hybrid minimum principle

Theorem ([28]). *Consider the hybrid system $\mathbb{H}$ subject to assumptions* A0–A2 *(in Appendix A), and the HOCP (A.3) for the hybrid performance function (5). Define the family of system Hamiltonians by*

$$H_q\left(x_q, \lambda_{q,0}, \lambda_q, u_q, t\right) = \lambda_{q,0}\, l_q\left(x_q, u_q, t\right) + \lambda_q^T f_q\left(x_q, u_q, t\right), \tag{6}$$

for $x_q \in \mathbb{R}^{n_q}$, $\lambda_{q,0} \in \mathbb{R}$, $\lambda_q \in \mathbb{R}^{n_q}$, $u_q \in U_q$, $q \in Q$. Then for the optimal switching sequence q^o and along the optimal trajectory x^o there exists constants $\lambda^o_{q_i,0} \geq 0$ and adjoint processes $\lambda^o_{q_i}$ such that $\left[\lambda^o_{q_i,0}, \lambda^{o\,T}_{q_i}\right] \neq 0$, and $x^o_{q_i}$ and $\lambda^o_{q_i}$ satisfy the following extended Hamiltonian canonical system

$$\dot{x}^o_q = \frac{\partial H_{q^o}}{\partial \lambda_q}\left(x^o_q, \lambda^o_{q,0}, \lambda^o_q, u^o_q, t\right), \tag{7}$$

$$\dot{\lambda}^o_q = -\frac{\partial H_{q^o}}{\partial x_q}\left(x^o_q, \lambda^o_{q,0}, \lambda^o_q, u^o_q, t\right), \tag{8}$$

almost everywhere $t \in \left[t_0, t_f\right]$ with

$$x^o_{q^o_0}(t_0) = x_0, \tag{9}$$

$$x^o_{q^o_{j-1}}\left(t_j-\right) \in m_j := \left\{x \in \mathbb{R}^{n_{q_{j-1}}} : m^1_{q_{j-1}q_j}(x) = 0 \wedge \cdots \wedge m^{k_j}_{q_{j-1}q_j}(x) = 0\right\}, \tag{10}$$

$$x^o_{q^o_j}\left(t_j\right) = \xi_{\sigma_j}\left(x^o_{q^o_{j-1}}\left(t_j-\right)\right), \tag{11}$$

$$x^o_{q^o_L}\left(t_f\right) \in m_f := \left\{x \in \mathbb{R}^{n_{q_L}} : m^1_{q_L,\text{stop}}(x) = 0 \wedge \cdots \wedge m^{k_{L+1}}_{q_L,\text{stop}}(x) = 0\right\}, \tag{12}$$

$$\lambda^o_{q^o_L}\left(t_f\right) = \nabla g\left(x^o_{q^o_L}\left(t_f\right)\right) + \sum_{i=1}^{k_{L+1}} p^i_{L+1} \nabla m^i_{L+1}\left(x^o_{q^o_L}\left(t_f\right)\right), \tag{13}$$

$$\lambda^o_{q^o_{j-1}}\left(t_j-\right) \equiv \lambda^o_{q^o_{j-1}}\left(t_j\right) = \nabla \xi_{\sigma_j}{}^T \lambda^o_{q^o_j}\left(t_j+\right) + \nabla c_{\sigma_j}\left(x^o_{q^o_{j-1}}\left(t_j-\right)\right) + \sum_{i=1}^{k_j} p^i_j \nabla m^i_j\left(x^o_{q^o_{j-1}}\left(t_j-\right)\right), \tag{14}$$

where $m_j = \emptyset$ and $p^i_j = 0$ when t_j indicates the time of a controlled switching and $p^i_j \in \mathbb{R}$ when t_j indicates the time of an autonomous switching.

Moreover,

$$H_{q^o}\left(x^o_q, \lambda^o_{q,0}, \lambda^o_q, u^o_q, t\right) \leq H_{q^o}\left(x^o_q, \lambda^o_{q,0}, \lambda^o_q, u, t\right), \tag{15}$$

for all $u \in U_{q^o}$, that is to say the Hamiltonian is minimized with respect to the control input, and at a switching time t_j the Hamiltonian satisfies

$$H_{q_{j-1}}\left(x^o_{q_{j-1}}, \lambda^o_{q_{j-1},0}, \lambda^o_{q_{j-1}}, u^o_{q_{j-1}}, t^o_j-\right) = H_{q_j}\left(x^o_{q_j}, \lambda^o_{q_j,0}, \lambda^o_{q_j}, u^o_{q_j}, t^o_j+\right) + \lambda^o_{q_j,0} \frac{\partial c\left(x^{o\,(t_j-)}_{q^o_{j-1}}\right)}{\partial t} + \sum_{i=1}^{k_j} p^i_j \frac{\partial m^i_j\left(x^{o\,(t_j-)}_{q^o_{j-1}}\right)}{\partial t} \tag{16}$$

where for the time invariant case, Eq. (16) becomes

$$H_{q^o_{j-1}}\left(x^o, \lambda^o_0, \lambda^o, u^o\right)\big|_{t_j-} \equiv H_{q^o_{j-1}}\left(t_j\right) = H_{q^o_j}\left(t_j\right) \equiv H_{q^o_j}\left(x^o, \lambda^o_0, \lambda^o, u^o\right)\big|_{t_j+}. \tag{17}$$

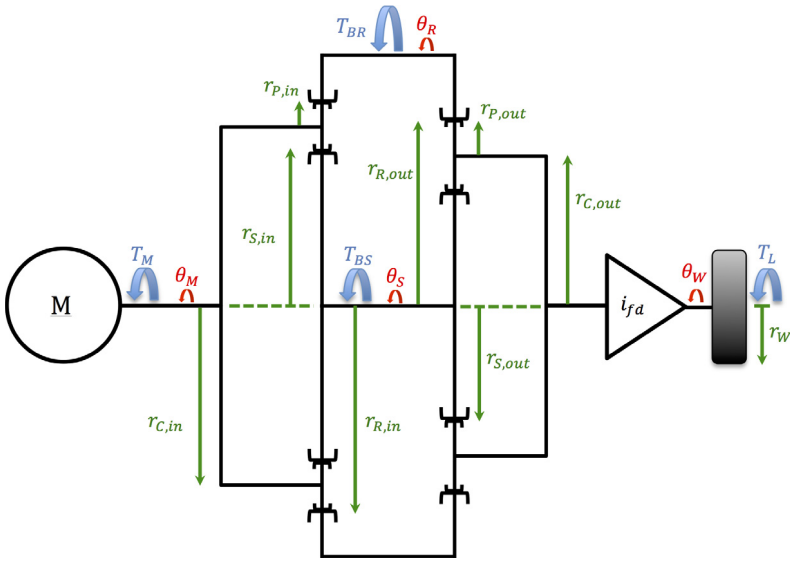

Fig. 1. A simplified model of the driveline of an EV equipped with the dual planetary transmission in [16,17].

For hybrid optimal control problems in which t_f is not fixed (i.e. not a priori specified), then

$$H_{q_f^o}\left(x_q^o, \lambda_{0,q}^o, \lambda_q^o, u_q^o\right)\Big|_{t_f^o} + \frac{\partial g\left(x_{q_L^o}^o\left(t_f\right)\right)}{\partial t} + \sum_{i=1}^{k_{L+1}} p_{L+1}^i \frac{m_{L+1}^i\left(x_{q_L^o}^o\left(t_f\right)\right)}{\partial t} = 0, \tag{18}$$

where for the time invariant case becomes

$$H_{q_f^o}\left(x_q^o, \lambda_{0,q}^o, \lambda_q^o, u_q^o\right)\Big|_{t_f^o} = 0. \quad \square \tag{19}$$

We note that the gradient of the state transition jump map $\nabla\xi_{\sigma_j}$ is not necessarily square due to the possibility of changes in the state dimension, but the boundary conditions (14) are well-defined for hybrid optimal control problems satisfying A0–A2 (in Appendix A).

The scalar $\lambda_{q_i,0}^o(t)$ is usually referred to as the abnormal multiplier (for more discussion about abnormality, see e.g. [29–31]) where it is zero for abnormal problems i.e. $\lambda_{q_i,0}^o(t) \equiv 0$, $0 \leq i \leq L$ (and therefore $\lambda_{q_i}^o(t) \neq 0$), and for normal problems, including the examples discussed in Sections 6 and 7, it is nonzero and therefore scalable to identity, i.e. $\lambda_{q_i,0}^o(t) \equiv 1$.

4. Electric vehicle with a dual-planetary transmission

The schematic view of the driveline of the electric vehicle under study is illustrated in Fig. 1. The power produced by the electric motor is transmitted to the wheels via a dual-stage planetary gear set with common ring and common sun gears, explained in more detail in [16,17]. The general configuration of the transmission mechanism has two degrees of freedom, providing different paths for the power flow. Brakes on the common sun gears and the common ring gears direct the power flow by locking the gears and eliminating their corresponding degree of freedom.

4.1. Driveline kinematics

With the consideration of the longitudinal coordinate z of a car moving on a road with an a priori known grading $\gamma(z)$, and assuming the zero-slippage condition on the wheels, the rotation angle of the wheel θ_W is related to z via

$$r_W\left(\theta_W - \theta_{W,0}\right) = z - z_0, \tag{20}$$

where r_W is the wheel radius and $\theta_{W,0}$ and z_0 are the initial values for θ_W and z respectively. Without loss of generality, it is assumed that the car's initial position is zero, i.e. $z_0 = 0$ and also the initial angles in the transmission are zero, i.e. $\theta_{W,0} = \theta_{S,0} = \theta_{R,0} = \theta_{C,in,0} = \theta_{C,out,0} = \theta_{P,in,0} = \theta_{P,out,0} = 0$, for simplicity of the notation. Taking the angle of the common sun gears θ_S and the angle of the common ring gears θ_R as the generalized coordinates of the system, other angles

Table 1
Values of the system parameters.

Parameter	Value	Unit	Parameter	Value	Unit
m	1000	kg	I_S	0.0015	kg m^2
ρ	1.2	$\frac{\text{kg}}{\text{m}^3}$	I_R	0.009	kg m^2
A_f	2	m^2	$I_{C,in}$	0.0014	kg m^2
C_d	0.3	–	$I_{C,out}$	0.1	kg m^2
C_r	0.02	–	$I_{P,in}$	6.08×10^{-6}	kg m^2
g	9.81	$\frac{\text{m}}{\text{s}^2}$	$I_{P,out}$	3.12×10^{-5}	kg m^2
i_{fd}	12	–	$m_{P,in}$	0.0512	kg
C_S	0.001	$\frac{\text{N m s}}{\text{rad}}$	$m_{P,out}$	0.12113	kg
C_R	0.001	$\frac{\text{N m s}}{\text{rad}}$	$r_{S,in}$	0.03	m
T_{Sf}	−0.05	N m	$r_{S,out}$	0.015	m
T_{Rf}	−0.05	N m	$r_{R,in}$	0.06	m
L_{TT}	0.1443	$\frac{1}{\text{N m s}}$	$r_{R,out}$	0.06	m
$L_{T\omega}$	1.014	–	$r_{P,in}$	0.015	m
L_T	−0.889	$\frac{1}{\text{s}}$	$r_{P,out}$	0.0225	m
L_ω	6.884	N m	r_W	0.3	m

of the components of the dual-stage planetary gear set as well as the car position are determined by the following kinematic relations (see also [16,17,27] for more detail):

$$\theta_M = \theta_{C,in} = \frac{1}{R_1 + 1}\theta_S + \frac{R_1}{R_1 + 1}\theta_R, \tag{21}$$

$$\theta_{C,out} = \frac{1}{R_2 + 1}\theta_S + \frac{R_2}{R_2 + 1}\theta_R, \tag{22}$$

$$z = \frac{r_W}{i_{fd}}\theta_{C,out} = \frac{r_W}{i_{fd}\,(R_2 + 1)}\theta_S + \frac{r_W R_2}{i_{fd}\,(R_2 + 1)}\theta_R, \tag{23}$$

$$\theta_{P,in} = \frac{-1}{R_1 - 1}\,\theta_S + \frac{R_1}{R_1 - 1}\,\theta_R, \tag{24}$$

$$\theta_{P,out} = \frac{-1}{R_2 - 1}\,\theta_S + \frac{R_2}{R_2 - 1}\,\theta_R, \tag{25}$$

where θ_M is the angle of the electric motor's rotor, $\theta_{C,in}$ and $\theta_{C,out}$ are respectively the angles of input and output carriers and, $\theta_{P,in}$ and $\theta_{P,out}$ are the angles of the planet gears connected to the input and output carriers respectively. In the above equations, i_{fd} is the gear ratio of differential and

$$R_2 := \frac{r_{R,out}}{r_{S,out}} > R_1 := \frac{r_{R,in}}{r_{S,in}} > 1, \tag{26}$$

holds with $r_{S,in}$, $r_{S,out}$ denoting the pitch radii of the sun gears in the input and output stages (see also Fig. 1), and $r_{R,in}$, $r_{R,out}$ denoting the pitch radii of the ring gears in the input and output stages respectively, whose values are presented in Table 1 (see also [16,17,27]).

It is worth noting that the time derivatives of the above angles, i.e. $v := \dot{z}$ and $\omega_M := \dot{\theta}_M$, etc. can be related to $\omega_S := \dot{\theta}_S$, $\omega_R := \dot{\theta}_R$ via the time differentiation of the above equations. In particular, in the first gear where the common ring gear is held fixed, i.e. $\omega_R = 0$, the time derivatives of (21) and (22) defines the first gear ratio of the transmission as

$$GR_1 := \left.\frac{\omega_{C,in}}{\omega_{C,out}}\right|_{\omega_R = 0} = \frac{R_2 + 1}{R_1 + 1}. \tag{27}$$

Similarly, the second gear corresponds to the configuration where the sun gear is locked, i.e. $\omega_S = 0$, and therefore

$$GR_2 := \left.\frac{\omega_{C,in}}{\omega_{C,out}}\right|_{\omega_S = 0} = \frac{(R_2 + 1)\,R_1}{(R_1 + 1)\,R_2}. \tag{28}$$

4.2. Dynamics of the powertrain

By the Principle of Virtual Work, the continuous evolution of the system is governed by the generalized Euler–Lagrange equation, i.e.

$$\frac{d}{dt}\frac{\partial L}{\partial \dot{q}_i} - \frac{\partial L}{\partial q_i} = D_i, \tag{29}$$

where q_i represents the ith component of the generalized coordinate, $L = T - V$ is the Lagrangian and D_i is the resultant of the generalized dissipative and driving forces acting on the generalized coordinate component q_i (see e.g. [32,33] for more discussion). In this paper $q \equiv [q_1, q_2]^T = [\theta_S, \theta_R]^T$ is selected as the generalized coordinates for the general configuration of the transmission (i.e. during the gear transition process) and $q = z$ is selected as the generalized coordinate for fixed gear configurations (i.e. the first and the second gears). The Kinetic Energy T of the system is written as

$$T = \frac{1}{2}\left(mv^2 + J_W\omega_W^2 + J_M\omega_M^2 + J_S\omega_S^2 + J_R\omega_R^2 + J_{P,in}\omega_{P,in}^2 + J_{P,out}\omega_{P,out}^2\right), \tag{30}$$

where m is the total mass of the vehicle, $J_W = 4I_W + I_{shaft} + i_{fd}^2\left(I_{C,out} + 4m_{P,out}r_{C,out}^2\right)$, is the equivalent inertia of the elements directly connected to the wheels, $J_M = I_M + I_{C,in} + 4m_{P,in}r_{C,in}^2$, is the equivalent inertia of the elements directly connected to the electric motor, J_S and J_R are respectively the inertia of the sun and the ring gears, and $J_{P,in} = 4I_{P,in}$ and $J_{P,out} = 4I_{P,out}$ are the total inertia of the input and output planetary sets respectively. The potential energy V consists only of the gravitational energy which is equivalent to

$$V = mg\Delta h = mg\int_{z_0}^{z} \sin\gamma\,(z)\,dz. \tag{31}$$

The virtual work of the generalized forces (see e.g. [32,33]) consists of the virtual work of the driving motor torque T_M and the brake torques T_{BS} and T_{BR} acting on the common sun and common ring gears respectively, the friction forces D_S and D_R acting on the sun and ring gears as well as the resistance force F_r on the displacement of the vehicle, described by the following variational equation

$$\delta W = \Sigma D_i\delta q_i = T_M\delta\theta_M + (T_{BS} + F_S)\,\delta\theta_S + (T_{BR} + F_R)\,\delta\theta_R + F_r\delta z, \tag{32}$$

where $F_r = -\frac{1}{2}\rho C_d A_f v^2 - mgC_r\cos\gamma\,(z)$ is the sum of the aerodynamic and rolling resistance forces and $F_S = -C_S\omega_S - T_{Sf}\,\mathrm{sign}\,(\omega_S)$ and $F_R = -C_R\omega_R - T_{Rf}\,\mathrm{sign}\,(\omega_R)$ are the sum of viscous and Coulomb frictions on the sun and ring gears. The dynamics in the first gear ($\omega_R = 0$) is derived in Appendix B.1 as

$$m_1^{eq}\dot{v} + mg\sin\gamma\,(z) = \frac{i_{fd}\,(R_2+1)}{r_W\,(R_1+1)}T_M - \frac{i_{fd}\,(R_2+1)}{r_W}T_{Sf} - \frac{i_{fd}^2\,(R_2+1)^2}{r_W^2}C_S v - \frac{1}{2}\rho C_d A_f v^2 - mgC_r\cos\gamma\,(z), \tag{33}$$

where $m_1^{eq} := m\left(1 + \frac{J_W}{mr_W^2} + \left(\frac{J_M}{(R_1+1)^2} + J_S + \frac{J_{P,in}}{(R_1-1)^2} + \frac{J_{P,out}}{(R_2-1)^2}\right)\frac{i_{fd}^2(R_2+1)^2}{mr_W^2}\right)$ is the equivalent mass in the first gear. The dynamics in the second gear ($\omega_S = 0$) is also found to be

$$m_2^{eq}\dot{v} - mg\sin\gamma\,(z) = \frac{i_{fd}\,(R_2+1)\,R_1}{r_W\,(R_1+1)\,R_2}T_M - \frac{i_{fd}\,(R_2+1)}{r_W R_2}T_{Rf} - \frac{i_{fd}^2\,(R_2+1)^2}{r_W^2 R_2^2}C_R v - \frac{1}{2}\rho C_d A_f v^2 - mgC_r\cos\gamma\,(z), \tag{34}$$

where $m_2^{eq} := m\left(1 + \frac{J_W}{mr_W^2} + \left(\frac{R_1^2 J_M}{(R_1+1)^2} + J_R + \frac{R_1^2 J_{P,in}}{(R_1-1)^2} + \frac{R_2^2 J_{P,out}}{(R_2-1)^2}\right)\frac{i_{fd}^2(R_2+1)^2}{mr_W^2 R_2^2}\right)$. In general, the above equations are coupled to $\dot{z} = v$ via the coupling term $-mg\sin\gamma\,(z)$. However, if the road has a negligible slope, i.e. $\sin\gamma\,(z) \approx 0$, then velocity becomes decoupled from the position, which is the case in the problems studied in this paper. The dynamics of the powertrain during the transition period ($\omega_S \neq 0$ and $\omega_R \neq 0$) is derived in Appendix B.2 as

$$\dot{\omega}_S = -A_{SS}\omega_S + A_{SR}\omega_R - A_{SA}\,(\omega_S + R_2\omega_R)^2 + B_{SS}T_{BS} - B_{SR}T_{BR} + B_{SM}T_M - D_{SL}, \tag{35}$$

$$\dot{\omega}_R = A_{RS}\omega_S - A_{RR}\omega_R - A_{RA}\,(\omega_S + R_2\omega_R)^2 - B_{RS}T_{BS} - B_{RR}T_{BR} + B_{RM}T_M - D_{RL}, \tag{36}$$

where the coefficients are introduced in Appendix B.2. We note that the brake torques T_{BS}, T_{BR} can only be resisting, i.e. $T_{BS} \in \left[-|T_{BS}|^{\max}, 0\right]$ and $T_{BR} \in \left[-|T_{BR}|^{\max}, 0\right]$.

4.3. Electric motor

The electric motor considered in this paper has specifications similar to the TM4 MOTIVE A® motor whose efficiency map $\eta\,(T_M, \omega_M)$ is illustrated in Fig. 2 and whose torque is constrained as a function of speed by

$$|T_M| \leq T_M^{\max} \tag{37}$$

and

$$|T_M\omega_M| \leq P_M^{\max} \tag{38}$$

with $T_M^{\max} = 200$ N m and $P_M^{\max} = 80$ kW.

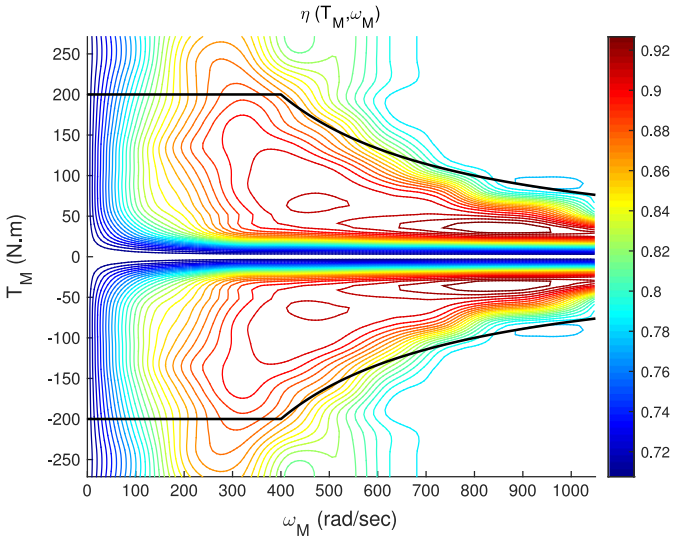

Fig. 2. Colour map: The electric motor efficiency map $\eta\,(T_M, \omega_M)$. Black curves: Torque constraint $\overline{T}_M$ as a function of the motor speed ω_M.

In order to avoid mixed state and input constraints like (38) we define a change of variable by the introduction of

$$u_1 = \frac{T_M}{T_M^{\max}}, \quad \omega_M < \omega^* \tag{39}$$

$$u_1 = \frac{T_M \omega_m}{P_M^{\max}}, \quad \omega_M \geq \omega^* \tag{40}$$

with $\omega^* = 400\ \frac{\text{rad}}{s}$. Thus the constraints (37) and (38) will both become $u_1 \in [-1, 1]$ which lies within the assumption A0 requiring U to be an invariant compact set.

The electric power consumed or generated corresponding to a pair (T_M, ω_M) is calculated as

$$P_b\,(T_M, \omega_M) = \begin{cases} \dfrac{T_M \cdot \omega_M}{\eta\,(T_M, \omega_M)} & T_M \omega_M \geq 0 \\ T_M \cdot \omega_M \cdot \eta\,(T_M, \omega_M) & T_M \omega_M < 0, \end{cases} \tag{41}$$

where $T_M \omega_M \geq 0$ corresponds to power consumption, $T_M \omega_M < 0$ indicates regeneration of power, and $\eta\,(T_M, \omega_M)$ is illustrated in Fig. 2.

In the analytical study of optimal control of electric vehicles (see e.g. [34,35]), it is customary to consider the following expression for the consumption of battery power by the motor

$$P_b\,(T_M, \omega_M) = L_{T\omega} T_M \omega_M + L_{TT} T_M^2 + L_T T_M + L_\omega \omega_M, \tag{42}$$

where the values of the parameters $L_{T\omega}, L_{TT}, L_T, L_\omega$ for the efficiency map in Fig. 2 are given in Table 1.

5. Hybrid systems formulation of the powertrain

In order to present the system dynamics in the hybrid framework presented in Section 2 and Appendix A, the following discrete states are assigned to each continuous dynamics of the system to form the hybrid automata diagram in Fig. 3:

Discrete states $\mathbf{q_1}$ and $\mathbf{q_2}$: We assign the discrete state q_1 to the torque constrained region of the first gear where the continuous state $x := v \in \mathbb{R}$ is such that the corresponding motor speed ω_M lies below ω^* and therefore, the motor torque is constrained by the maximum torque value. The vector field corresponding to q_1 is determined from (33) and the input is normalized by (39), which results in

$$\dot{x} = f_1\,(x, u) = -A_1 x^2 + B_1 u - C_1 x - D_1, \tag{43}$$

where

$$A_1 = \frac{\rho_a C_d A_f}{2 m_1^{eq}}, \qquad B_1 = \frac{i_{fd} G R_1 T_M^{\max}}{m_1^{eq} r_W}, \qquad C_1 = \frac{i_{fd}^2\,(R_2 + 1)^2\,C_S}{m_1^{eq} r_W^2}, \qquad D_1 = \frac{mgC_r}{m_1^{eq}}. \tag{44}$$

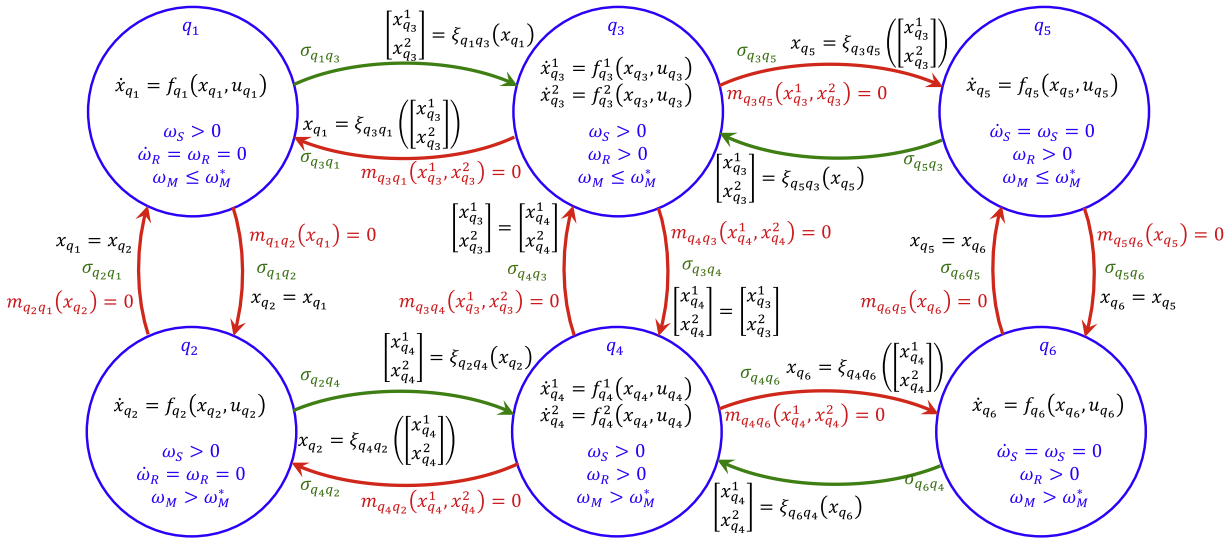

Fig. 3. Hybrid automata diagram for the driveline of an EV equipped with the dual planetary transmission.

When the motor speed $\omega_M = \frac{i_{fd} G R_1 v}{R_w}$ reaches $\omega^* = 400$ rad/s the system autonomously switches to q_2 with $x = v \in \mathbb{R}$ which corresponds to the dynamics in the power constrained region of the first gear. The vector field in this region is determined from (33) and the input is normalized by (40), which gives

$$\dot{x} = f_2(x, u) = -A_2 x^2 + B_2 \frac{u}{x} - C_2 x - D_2, \tag{45}$$

with

$$A_2 = A_1, \qquad B_2 = \frac{P_M^{\max}}{m_1^{eq}}, \qquad C_2 = C_1, \qquad D_2 = D_1. \tag{46}$$

The switching manifolds $m_{q_1q_2}$ and $m_{q_2q_1}$ are represented by

$$m_{q_1q_2}(x) = m_{q_2q_1}(x) \equiv x - \frac{\omega^* R_w}{i_{fd} G R_1} = 0. \tag{47}$$

Discrete states q_3 and q_4: During the gear changing process, if the motor speed is lower than ω^* the input torque is limited by the maximum torque to which we assign the discrete state q_3. The continuous state $x = [\omega_S, \omega_R]^T \in \mathbb{R}^2$ is governed by the powertrain dynamics (35) and (36) and by the normalization of the motor torque (39) and the brake toques $u_2 := T_{BS}/|T_{BS}|^{\max}$ and $u_3 := T_{BR}/|T_{BR}|^{\max}$, the vector field is described by

$$\dot{x} = f_3(x, u), \tag{48}$$

where

$$\dot{x}_1 = f_3^{(1)}(x, u) = -A_{SS} x_1 + A_{SR} x_2 - A_{SA}(x_1 + R_2 x_2)^2 + B_{SM} T_M^{\max} u_1 + B_{SS} |T_{BS}|^{\max} u_2 - B_{SR} |T_{BR}|^{\max} u_3 - D_{SL}, \tag{49}$$

$$\dot{x}_2 = f_3^{(2)}(x, u) = A_{RS} x_1 - A_{RR} x_2 - A_{RA}(x_1 + R_2 x_2)^2 + B_{RM} T_M^{\max} u_1 - B_{RS} |T_{BS}|^{\max} u_2 - B_{RR} |T_{BR}|^{\max} u_3 - D_{RL}, \tag{50}$$

and where $u_1 \in [-1, 1]$ is the normalized motor torque in the torque constraint region, and $u_2, u_3 \in [-1, 0]$ are respectively the normalized sun brake and the normalized ring brake torques.

We assign q_4 with $x = [\omega_S, \omega_R]^T \in \mathbb{R}^2$ to the dynamics in the power constraint region during the gear changing with the vector field

$$\dot{x} = f_4(x, u), \tag{51}$$

where

$$\begin{aligned} \dot{x}_1 &= f_4^{(1)}(x, u) = -A_{SS} x_1 + A_{SR} x_2 - A_{SA}(x_1 + R_2 x_2)^2 \\ &\quad + B_{SM} P_M^{\max}(1 + R_1) \frac{u_1}{x_1 + R_1 x_2} + B_{SS} |T_{BS}|^{\max} u_2 - B_{SR} |T_{BR}|^{\max} u_3 - D_{SL}, \end{aligned} \tag{52}$$

$$\begin{aligned} \dot{x}_2 &= f_4^{(2)}(x, u) = A_{RS} x_1 - A_{RR} x_2 - A_{RA}(x_1 + R_2 x_2)^2 \\ &\quad + B_{RM} P_M^{\max}(1 + R_1) \frac{u_1}{x_1 + R_1 x_2} - B_{RS} |T_{BS}|^{\max} u_2 + B_{RR} |T_{BR}|^{\max} u_3 - D_{RL}. \end{aligned} \tag{53}$$

The jump map corresponding to the (controlled) transitions from q_1 to q_3 and from q_2 to q_4 are described by $\xi_{q_1q_3} : \mathbb{R} \to \mathbb{R}^2$ and $\xi_{q_2q_4} : \mathbb{R} \to \mathbb{R}^2$ in the form of

$$x(t_s) = \xi_{q_1q_3}(x(t_s-)) = \frac{i_{fd}(1+R_2)}{r_W}\begin{bmatrix}1\\0\end{bmatrix} x(t_s-), \tag{54}$$

$$x(t_s) = \xi_{q_2q_4}(x(t_s-)) = \frac{i_{fd}(1+R_2)}{r_W}\begin{bmatrix}1\\0\end{bmatrix} x(t_s-). \tag{55}$$

Note, however, that the transitions back to q_1 from q_3 and to q_2 from q_4 are autonomous with the switching manifolds described by

$$m_{q_3q_1}(x) \equiv x_2 = 0, \tag{56}$$

$$m_{q_4q_2}(x) \equiv x_2 = 0, \tag{57}$$

i.e. when the ring gear comes to a full stop. The autonomous transition between q_3 and q_4 is constrained to the switching manifold condition

$$m_{q_3q_4}(x) = m_{q_4q_3}(x) \equiv \frac{x_1 + R_1x_2}{R_1+1} - \omega^* = 0, \tag{58}$$

with both jump transition maps $\xi_{q_3q_4}, \xi_{q_4q_3} : \mathbb{R}^2 \to \mathbb{R}^2$ being identity.

Discrete states q_5 and q_6: When the speed of the sun gear ω_S becomes zero the system switches to q_5 or q_6 (depending on the corresponding motor speed) with $x = v \in \mathbb{R}$ where q_5 corresponds to the dynamics in the torque constraint region of the second gear and q_6 corresponds to the dynamics in the power constraint region of the second gear. The corresponding vector fields are described by

$$\dot{x} = f_5(x,u) = -A_5x^2 + B_5u - C_5x - D_5, \tag{59}$$

and

$$\dot{x} = f_6(x,u) = -A_6x^2 + B_6\frac{u}{x} - C_6x - D_6, \tag{60}$$

where

$$A_5 = A_6 = \frac{\rho_a C_d A_f}{2m_2^{eq}}, \qquad B_5 = \frac{i_{fd}GR_2T_M^{\max}}{m_2^{eq}r_W} \qquad B_6 = \frac{P_M^{\max}}{m_2^{eq}}, \qquad C_5 = C_6 = \frac{i_{fd}^2(R_2+1)^2C_S}{m_2^{eq}r_W^2}, \qquad D_5 = D_6 = \frac{mgC_r}{m_1^{eq}}. \tag{61}$$

The switching manifold corresponding to the transition from q_3 to q_5 and from q_4 to q_6 are described as

$$m_{q_3q_5}(x) \equiv x_1 = 0, \tag{62}$$

$$m_{q_4q_6}(x) \equiv x_1 = 0, \tag{63}$$

and the jump map corresponding to these transitions are given by

$$x(t_s) = \xi_{q_3q_5}(x(t_s-)) = \frac{r_W}{i_{fd}(1+R_2)}\begin{bmatrix}1 & R_2\end{bmatrix} x(t_s-), \tag{64}$$

$$x(t_s) = \xi_{q_4q_6}(x(t_s-)) = \frac{r_W}{i_{fd}(1+R_2)}\begin{bmatrix}1 & R_2\end{bmatrix} x(t_s-), \tag{65}$$

with $\xi_{q_3q_5} : \mathbb{R}^2 \to \mathbb{R}$ and $\xi_{q_4q_6} : \mathbb{R}^2 \to \mathbb{R}$.

6. Acceleration within the minimum time interval

First, consider the hybrid optimal control problem for the minimization of the acceleration period required for reaching the top speed of 100 $\frac{\text{km}}{\text{h}} = 27.78\ \frac{\text{m}}{\text{s}} \approx 60$ mph. The vehicle is assumed to start from the stationary state in the first gear which corresponds to q_1, autonomously switch to the torque constraint region q_2, then switch to the gear transition phase initiated by a controlled switching command σ_{q_2,q_4} and finally, reach the terminal state $x_f = 27.78\ \frac{\text{m}}{\text{s}}$ in the power constraint region of the second gear q_6.

The cost to be minimized is

$$J\left(u, T_{BS}, T_{BR}; t_{s_1}, t_{s_2}, t_{s_3}\right) = \int_{t_0}^{t_{s_1}} dt + \int_{t_{s_1}}^{t_{s_2}} dt + \int_{t_{s_2}}^{t_{s_3}} dt + \int_{t_{s_3}}^{t_f} dt, \tag{66}$$

with t_f being the first time that $x(t) = 27.78$ is satisfied.

Formation of the Hamiltonians: It can easily be verified that the problem under study is normal and therefore, the abnormal multiplier can be normalized to unity, i.e. $\lambda^o_{q_k,0}(t) = 1, k = 1, 2, 4, 6$. Hence, the family of system Hamiltonians is formed as

$$H_{q_1}(x, \lambda, u) = 1 + \lambda\left(-A_1x^2 + B_1u - C_1x - D_1\right), \tag{67}$$

$$H_{q_2}(x, \lambda, u) = 1 + \lambda\left(-A_2x^2 + B_2\frac{u}{x} - C_2x - D_2\right), \tag{68}$$

$$\begin{aligned} H_{q_4}(x, \lambda, u, T_{BS}, T_{BR}) &= 1 \\ &+ \lambda_1\left(-A_{SS}x_1 + A_{SR}x_2 - A_{SA}(x_1 + R_2x_2)^2 + B_{SM}P_M^{\max}(1 + R_1)\frac{u_1}{x_1 + R_1x_2} + B_{SS}|T_{BS}|^{\max}u_2 - B_{SR}|T_{BR}|^{\max}u_3 - D_{SL}\right) \\ &+ \lambda_2\left(A_{RS}x_1 - A_{RR}x_2 - A_{RA}(x_1 + R_2x_2)^2 + B_{RM}P_M^{\max}(1 + R_1)\frac{u_1}{x_1 + R_1x_2} - B_{RS}|T_{BS}|^{\max}u_2 + B_{RR}|T_{BR}|^{\max}u_3 - D_{RL}\right), \end{aligned} \tag{69}$$

$$H_{q_6}(x, \lambda, u) = 1 + \lambda\left(-A_6x^2 + B_6\frac{u}{x} - C_6x - D_6\right). \tag{70}$$

Hamiltonian minimization: The Hamiltonian minimization condition (15) results in $u^o = 1, t \in [t_0, t_f]$, $T^o_{BS} = -|T_{BS}|^{\max}$ and $T^o_{BR} = 0$ for $t \in [t_{s_2}, t_{s_3}]$ wherever the adjoint process has a negative sign. The strict negative sign for the adjoint process is later confirmed for all $t \in [t_0, t_f]$ in the numerical solution (see Fig. 4).

Continuous state evolution: The continuous state dynamics (7) are equivalent to (43), (45), (51) and (60) subject to the stationary initial, boundary and terminal conditions

$$x(t_0) = x(0) = 0, \tag{71}$$

$$x(t_{s_1}) = \xi_{q_1q_2}(x(t_{s_1}-)) = x(t_{s_1}-), \tag{72}$$

$$x(t_{s_2}) = \xi_{q_2q_4}(x(t_{s_2}-)) = \frac{i_{fd}(1 + R_2)}{r_W}\begin{bmatrix}1\\0\end{bmatrix}x(t_{s_2}-), \tag{73}$$

$$x(t_{s_3}) = \xi_{q_4q_6}(x(t_{s_3}-)) = \frac{r_W}{i_{fd}(1 + R_2)}\begin{bmatrix}1 & R_2\end{bmatrix}x(t_{s_3}-), \tag{74}$$

$$x(t_f) = 27.78 \tag{75}$$

and where the transitions from q_1 to q_2 and from q_4 to q_6 are subject to the switching manifold conditions

$$m_{q_1q_2}(x(t_{s_1}-)) \equiv x(t_{s_1}-) - \frac{\omega^*R_w}{i_{fd}GR_1} = 0, \tag{76}$$

$$m_{q_4q_6}(x(t_{s_3}-)) \equiv x_1(t_{s_3}-) = 0. \tag{77}$$

Evolution of the adjoint process: According to the Hybrid Minimum Principle in Section 3:

$$\dot\lambda = \frac{-\partial H_{q_1}}{\partial x} = -(-2A_1x - C_1)\lambda, \quad t \in [t_0, t_{s_1}] \tag{78}$$

$$\dot\lambda = \frac{-\partial H_{q_2}}{\partial x} = -\left(-2A_2x - B_2\frac{u^o}{x^2} - C_2\right)\lambda, \quad t \in (t_{s_1}, t_{s_2}] \tag{79}$$

$$\dot\lambda = \frac{-\partial H_{q_4}}{\partial x}, \quad t \in (t_{s_2}, t_{s_3}], \tag{80}$$

with

$$\begin{aligned} \dot\lambda_1 &= \frac{-\partial H_{q_4}}{\partial x_1} = -\lambda_1\left(-A_{SS} - 2A_{SA}(x_1 + R_2x_2) - \frac{B_{SM}P_M^{\max}(1 + R_1)u_1}{(x_1 + R_1x_2)^2}\right) \\ &\quad - \lambda_2\left(A_{RS} - 2A_{RA}(x_1 + R_2x_2) - \frac{B_{RM}P_M^{\max}(1 + R_1)u_1}{(x_1 + R_1x_2)^2}\right), \end{aligned} \tag{81}$$

$$\begin{aligned} \dot\lambda_2 &= \frac{-\partial H_{q_4}}{\partial x_2} = -\lambda_1\left(A_{SR} - 2R_2A_{SA}(x_1 + R_2x_2) - \frac{R_1B_{SM}P_M^{\max}(1 + R_1)u_1}{(x_1 + R_1x_2)^2}\right) \\ &\quad - \lambda_2\left(-A_{RR} - 2R_2A_{RA}(x_1 + R_2x_2) - \frac{R_1B_{RM}P_M^{\max}(1 + R_1)u_1}{(x_1 + R_1x_2)^2}\right), \end{aligned} \tag{82}$$

and

$$\dot\lambda = \frac{-\partial H_{q_6}}{\partial x} = -\left(-2A_6x - B_6\frac{u^o}{x^2} - C_6\right)\lambda, \quad t \in (t_{s_3}, t_f]. \tag{83}$$

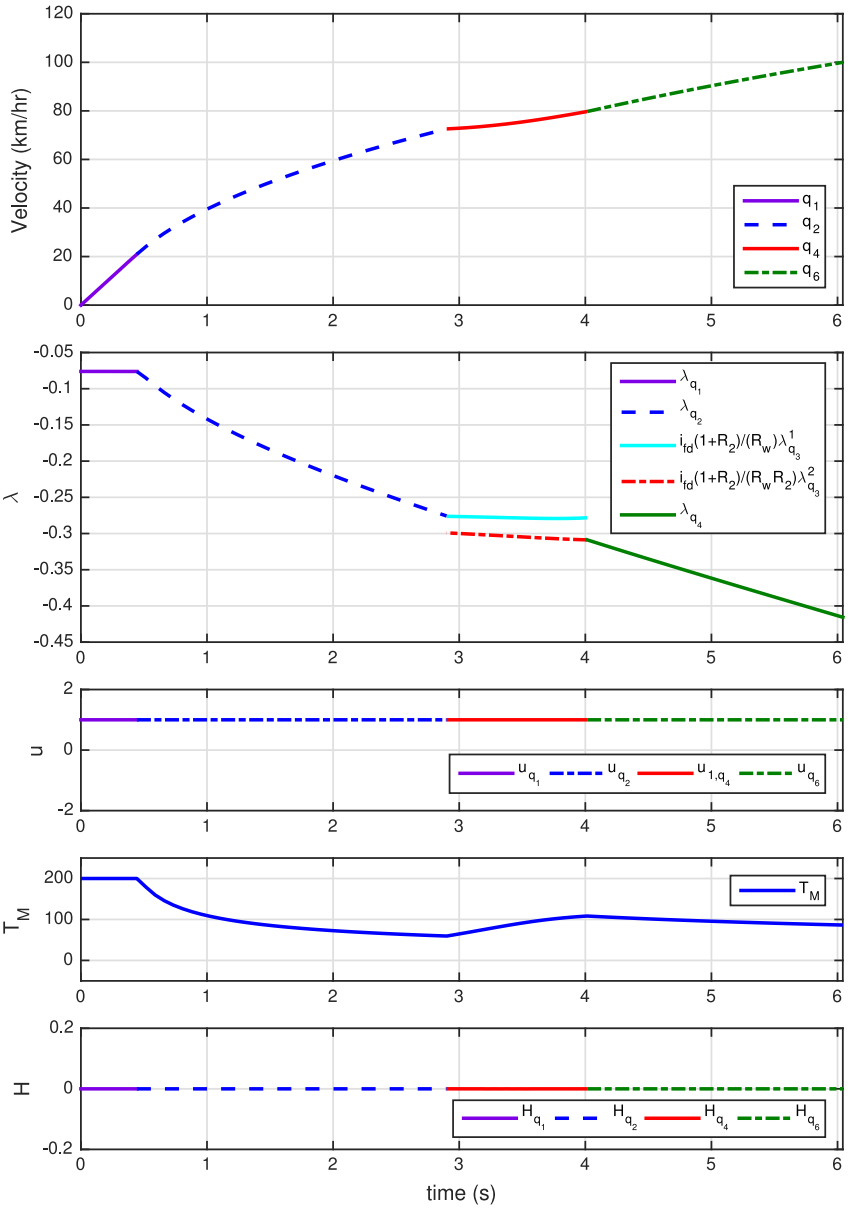

Fig. 4. The car speed, the adjoint processes and the corresponding Hamiltonians for the minimum acceleration period problem.

The boundary conditions for λ are determined from Eq. (14) as

$$\lambda\left(t_{s_3}\right) = \nabla\xi^T_{q_3q_4}\lambda\left(t_{s_3}+\right) + p_3\nabla m_{q_3q_4} = \frac{R_w}{i_{fd}\left(1+R_2\right)}\begin{bmatrix}1\\R_2\end{bmatrix}\lambda\left(t_{s_3}+\right) + p_3\begin{bmatrix}1\\0\end{bmatrix}, \tag{84}$$

$$\lambda\left(t_{s_2}\right) = \nabla\xi^T_{q_2q_3}\lambda\left(t_{s_2}+\right) = \frac{i_{fd}\left(1+R_2\right)}{R_w}\begin{bmatrix}1 & 0\end{bmatrix}\lambda\left(t_{s_2}+\right), \tag{85}$$

$$\lambda\left(t_{s_1}\right) = \lambda\left(t_{s_1}+\right) + p_1. \tag{86}$$

Boundary conditions on Hamiltonians: Since the terminal time is not a priori specified in this minimum time acceleration task, the Hamiltonian terminal condition (19) determines the Hamiltonian terminal condition

$$H_{q_6}\left(x,\lambda,u\right)_{(t_f)} = 1 + \lambda\left(t_f\right)\left(-A_6x\left(t_f\right)^2 - B_6\frac{u\left(t_f\right)}{x\left(t_f\right)} - C_6x\left(t_f\right) - D_6\right) = 0, \tag{87}$$

and the Hamiltonian continuity at switching instants is deduced from (17) as

$$H_{q_4}(x,\lambda,u)_{(t_{s_3}-)} = H_{q_6}(x,\lambda,u)_{(t_{s_3}+)}, \tag{88}$$

$$H_{q_2}(x,\lambda,u)_{(t_{s_2}-)} = H_{q_4}(x,\lambda,u)_{(t_{s_2}+)}, \tag{89}$$

$$H_{q_1}(x,\lambda,u)_{(t_{s_1}-)} = H_{q_2}(x,\lambda,u)_{(t_{s_1}+)}. \tag{90}$$

Numerical results: The results for the parameter values presented in Table 1 are illustrated in Fig. 4. For better illustration, the speed of the vehicle is shown in km/hr units and in addition, the components λ_1 and λ_2 of the adjoint process in $t \in [t_{s_2}, t_{s_3}]$ are multiplied by $i_{fd}(1+R_2)/R_w$ and $i_{fd}(1+R_2)/(R_wR_2)$ respectively so that the boundary conditions (121) and (122) can be verified more easily. The optimal values for the switching and final times are $t_{s_1} = 0.444$, $t_{s_2} = 2.901$, $t_{s_3} = 4.014$, $t_f = 6.042$.

7. Acceleration with the minimum energy

Now, consider the hybrid optimal control problem for the minimization of energy required for reaching the top speed of $100\ \frac{\text{km}}{\text{h}} = 27.78\ \frac{\text{m}}{\text{s}}$ at $t_f = 6.3$ s, which is slightly longer than the minimum time 6.042 s found in Section 6. The vehicle is assumed to start from the stationary state in the first gear which corresponds to q_1, autonomously switch to the torque constraint region q_2, then switch to the gear transition phase initiated by a controlled switching command σ_{q_2,q_4} and finally, reach the terminal state $x_f = 27.78\ \frac{\text{m}}{\text{s}}$ at $t_f = 6.3$ in the power constraint region of the second gear q_6. The cost to be minimized is the total electric energy consumed from the battery, i.e.

$$\begin{aligned} J\left(t_0, t_f, (q_1,0), 3; I_3\right) &= \int_{t_0}^{t_f} P_b(T_M, \omega_M)\, dt \\ &= \int_{t_0}^{t_{s_1}} l_{q_1}(x,u)\, dt + \int_{t_{s_1}}^{t_{s_2}} l_{q_2}(x,u)\, dt + \int_{t_{s_2}}^{t_{s_3}} l_{q_4}(x,u)\, dt + \int_{t_{s_3}}^{t_f} l_{q_6}(x,u)\, dt, \end{aligned} \tag{91}$$

where

$$l_{q_1}(x,u) = a_1u^2 + b_1xu + c_1u + d_1x, \tag{92}$$

$$l_{q_2}(x,u) = a_2\frac{u^2}{x^2} + b_2u + c_2\frac{u}{x} + d_2x, \tag{93}$$

$$l_{q_4}(x,u) = a_4\frac{u_1^2}{(x_1+R_1x_2)^2} + b_4u_1 + c_4\frac{u_1}{x_1+R_1x_2} + d_4(x_1+R_1x_2), \tag{94}$$

$$l_{q_6}(x,u) = a_6\frac{u^2}{x^2} + b_6u + c_6\frac{u}{x} + d_6x, \tag{95}$$

and where in the above equations

$$a_1 = L_{TT}\left(T_M^{\max}\right)^2, \quad b_1 = L_{T\omega}\frac{i_{fd}GR_1T_M^{\max}}{r_W}, \quad c_1 = L_TT_M^{\max}, \quad d_1 = L_\omega\frac{i_{fd}GR_1}{r_W}, \tag{96}$$

$$a_2 = L_{TT}\left(\frac{r_WP_M^{\max}}{i_{fd}GR_1}\right)^2, \quad b_2 = L_{T\omega}P_M^{\max}, \quad c_2 = L_T\left(\frac{r_WP_M^{\max}}{i_{fd}GR_1}\right), \quad d_2 = L_\omega\frac{i_{fd}GR_1}{r_W}, \tag{97}$$

$$a_4 = L_{TT}\left(P_M^{\max}\right)^2(R_1+1)^2, \quad b_4 = L_{T\omega}P_M^{\max}, \quad c_4 = L_TP_M^{\max}(R_1+1), \quad d_4 = \frac{L_\omega}{R_1+1}, \tag{98}$$

$$a_6 = L_{TT}\left(\frac{r_WP_M^{\max}}{i_{fd}GR_2}\right)^2, \quad b_6 = L_{T\omega}P_M^{\max}, \quad c_6 = L_T\left(\frac{r_WP_M^{\max}}{i_{fd}GR_2}\right), \quad d_6 = L_\omega\frac{i_{fd}GR_2}{r_W}. \tag{99}$$

Formation of the Hamiltonians: The family of system Hamiltonians is formed as

$$H_{q_1}(x,\lambda,u) = a_1u^2 + b_1xu + c_1u + d_1x + \lambda\left(-A_1x^2 + B_1u - C_1x - D_1\right) \tag{100}$$

$$H_{q_2}(x,\lambda,u) = a_2\frac{u^2}{x^2} + b_2u + c_2\frac{u}{x} + d_2x + \lambda\left(-A_2x^2 + B_2\frac{u}{x} - C_2x - D_2\right) \tag{101}$$

$$H_{q_4}(x,\lambda,u) = a_4\frac{u_1^2}{(x_1+R_1x_2)^2} + b_4u_1 + c_4\frac{u_1}{x_1+R_1x_2} + d_4(x_1+R_1x_2)$$

$$+\lambda_1\left(-A_{SS}x_1+A_{SR}x_2-A_{SA}\left(x_1+R_2x_2\right)^2+B_{SM}P_M^{\max}\left(1+R_1\right)\frac{u_1}{x_1+R_1x_2}+B_{SS}\left|T_{BS}\right|^{\max}u_2-B_{SR}\left|T_{BR}\right|^{\max}u_3-D_{SL}\right)$$

$$+\lambda_2\left(A_{RS}x_1-A_{RR}x_2-A_{RA}\left(x_1+R_2x_2\right)^2+B_{RM}P_M^{\max}\left(1+R_1\right)\frac{u_1}{x_1+R_1x_2}-B_{RS}\left|T_{BS}\right|^{\max}u_2+B_{RR}\left|T_{BR}\right|^{\max}u_3-D_{RL}\right), \quad (102)$$

and

$$H_{q_6}\left(x,\lambda,u\right)=a_6\frac{u^2}{x^2}+b_6u+c_6\frac{u}{x}+d_6x+\lambda\left(-A_6x^2+B_6\frac{u}{x}-C_6x-D_6\right). \quad (103)$$

Hamiltonian minimization: The Hamiltonian minimization condition (15) gives

$$u_{q_1}^o=\mathrm{sat}_{[-1,1]}\left(\frac{-\left(b_1x+c_1+B_1\lambda\right)}{2a_1}\right), \quad (104)$$

$$u_{q_2}^o=\mathrm{sat}_{[-1,1]}\left(\frac{-x\left(b_2x+c_2+B_2\lambda\right)}{2a_2}\right), \quad (105)$$

$$u_{1,q_4}^o=\mathrm{sat}_{[-1,1]}\left(\frac{-\left(x_1+R_1x_2\right)\left[b_4\left(x_1+R_1x_2\right)+c_4+B_{SM}P_M^{\max}\left(1+R_1\right)\lambda_1+B_{RM}P_M^{\max}\left(1+R_1\right)\lambda_2\right]}{2a_4}\right),$$

$$u_{2,q_4}^o=\begin{cases}-1 & \text{if} \quad B_{SS}\lambda_1-B_{RS}\lambda_2\geq 0\\ 0 & \text{if} \quad B_{SS}\lambda_1-B_{RS}\lambda_2<0,\end{cases} \quad (106)$$

$$u_{3,q_4}^o=\begin{cases}-1 & \text{if} \quad B_{RR}\lambda_2-B_{SR}\lambda_1\geq 0\\ 0 & \text{if} \quad B_{RR}\lambda_2-B_{SR}\lambda_1<0,\end{cases}$$

$$u_{q_6}^o=\mathrm{sat}_{[-1,1]}\left(\frac{-x\left(b_6x+c_6+B_6\lambda\right)}{2a_6}\right). \quad (107)$$

Continuous state evolution: The continuous state dynamics (7) are equivalent to (43), (45), (51) and (60) subject to the stationary initial, boundary and terminal conditions

$$x\left(t_0\right)=x\left(0\right)=0, \quad (108)$$

$$x\left(t_{s_1}\right)=\xi_{q_1q_2}\left(x\left(t_{s_1}-\right)\right)=x\left(t_{s_1}-\right), \quad (109)$$

$$x\left(t_{s_2}\right)=\xi_{q_2q_4}\left(x\left(t_{s_2}-\right)\right)=\frac{i_{fd}\left(1+R_2\right)}{r_W}\begin{bmatrix}1\\0\end{bmatrix}x\left(t_{s_2}-\right), \quad (110)$$

$$x\left(t_{s_3}\right)=\xi_{q_4q_6}\left(x\left(t_{s_3}-\right)\right)=\frac{r_W}{i_{fd}\left(1+R_2\right)}\begin{bmatrix}1 & R_2\end{bmatrix}x\left(t_{s_3}-\right), \quad (111)$$

$$x\left(t_f\right)=x\left(6.3\right)=27.78 \quad (112)$$

and where the transitions from q_1 to q_2 and from q_4 to q_6 are subject to the switching manifold conditions

$$m_{q_1q_2}\left(x\left(t_{s_1}-\right)\right)\equiv x\left(t_{s_1}-\right)-\frac{\omega^*R_w}{i_{fd}GR_1}=0, \quad (113)$$

$$m_{q_4q_6}\left(x\left(t_{s_3}-\right)\right)\equiv x_1\left(t_{s_3}-\right)=0. \quad (114)$$

Evolution of the adjoint process: The adjoint process dynamics (8) are governed by

$$\dot{\lambda}=\frac{-\partial H_{q_1}}{\partial x}=-\left(b_1u+d_1+\lambda\left(-2A_1x-C_1\right)\right), \quad t\in\left[t_0,t_{s_1}\right], \quad (115)$$

$$\dot{\lambda}=\frac{-\partial H_{q_2}}{\partial x}=-\left(\frac{-2a_2u^2}{x^3}-\frac{c_2u}{x^2}+d_2+\lambda\left(-2A_2x-B_2\frac{u^o}{x^2}-C_2\right)\right), \quad t\in\left(t_{s_1},t_{s_2}\right], \quad (116)$$

$$\dot{\lambda}=\frac{-\partial H_{q_4}}{\partial x}, \quad t\in\left(t_{s_2},t_{s_3}\right], \quad (117)$$

with

$$\begin{aligned}\dot{\lambda}_1=\frac{-\partial H_{q_4}}{\partial x_1}&=-\left(\frac{-2a_4u_1^2}{\left(x_1+R_1x_2\right)^3}-\frac{c_4u_1}{\left(x_1+R_1x_2\right)^2}+d_4\right)\\&-\lambda_1\left(-A_{SS}-2A_{SA}\left(x_1+R_2x_2\right)-\frac{B_{SM}P_M^{\max}\left(1+R_1\right)u_1}{\left(x_1+R_1x_2\right)^2}\right)\\&-\lambda_2\left(A_{RS}-2A_{RA}\left(x_1+R_2x_2\right)-\frac{B_{RM}P_M^{\max}\left(1+R_1\right)u_1}{\left(x_1+R_1x_2\right)^2}\right),\end{aligned} \quad (118)$$

$$\begin{aligned}\dot{\lambda}_2 &= \frac{-\partial H_{q_4}}{\partial x_2} = -\left(\frac{-2R_1a_4u_1^2}{(x_1+R_1x_2)^3} - \frac{R_1c_4u_1}{(x_1+R_1x_2)^2} + R_1d_4\right)\\ &\quad -\lambda_1\left(A_{SR} - 2R_2A_{SA}(x_1+R_2x_2) - \frac{R_1B_{SM}P_M^{\max}(1+R_1)u_1}{(x_1+R_1x_2)^2}\right)\\ &\quad -\lambda_2\left(-A_{RR} - 2R_2A_{RA}(x_1+R_2x_2) - \frac{R_1B_{RM}P_M^{\max}(1+R_1)u_1}{(x_1+R_1x_2)^2}\right),\end{aligned} \tag{119}$$

and

$$\dot{\lambda} = \frac{-\partial H_{q_6}}{\partial x} = -\left(\frac{-2a_6u^2}{x^3} - \frac{c_6u}{x^2} + d_6 + \lambda\left(-2A_6x - B_6\frac{u^o}{x^2} - C_6\right)\right), \quad t \in \left(t_{s_3}, t_f\right], \tag{120}$$

subject to the boundary condition determined from Eq. (14) as

$$\lambda\left(t_{s_3}\right) = \nabla\xi^T_{q_4q_6}\lambda\left(t_{s_3}+\right) + p_3\nabla m_{q_3q_4} = \frac{R_w}{i_{fd}(1+R_2)}\begin{bmatrix}1\\R_2\end{bmatrix}\lambda\left(t_{s_3}+\right) + p_3\begin{bmatrix}1\\0\end{bmatrix}, \tag{121}$$

$$\lambda\left(t_{s_2}\right) = \nabla\xi^T_{q_2q_4}\lambda\left(t_{s_2}+\right) = \frac{i_{fd}(1+R_2)}{R_w}\begin{bmatrix}1 & 0\end{bmatrix}\lambda\left(t_{s_2}+\right), \tag{122}$$

$$\lambda\left(t_{s_1}\right) = \nabla\xi^T_{q_1q_2}\lambda\left(t_{s_1}+\right) + p_1 = \lambda\left(t_{s_1}+\right) + p_1. \tag{123}$$

Boundary conditions on Hamiltonians: Furthermore, the Hamiltonian continuity at switching instants is deduced from (17) as

$$H_{q_4}(x,\lambda,u)_{(t_{s_3}-)} = H_{q_6}(x,\lambda,u)_{(t_{s_3}+)}, \tag{124}$$

$$H_{q_2}(x,\lambda,u)_{(t_{s_2}-)} = H_{q_4}(x,\lambda,u)_{(t_{s_2}+)}, \tag{125}$$

$$H_{q_1}(x,\lambda,u)_{(t_{s_1}-)} = H_{q_2}(x,\lambda,u)_{(t_{s_1}+)}. \quad \square \tag{126}$$

Numerical results: The results for the parameter values listed in Table 1 are illustrated in Fig. 5. A phenomenon of special interest that appears in the results is that the optimal control for the minimization of energy consumption coincides with a regeneration of power during the shifting period. This is in contrast with the inputs for the shifting period of the acceleration task in Section 6 and in [27] in which the motor produces power at the full rate to reach the top speed in the minimum time possible, and also in contrast with the task of smooth gear changing in [16,17] with (almost) no speed drop. The presence of power regeneration in the currently studied example, not only contributes to the saving of electric energy, but also contributes to the significant decrease of shifting duration from around 1 s in [16,17,27] to 0.1058 s.

In order to illustrate the satisfaction of the adjoint boundary conditions (121) and (122), the components λ_1 and λ_2 of the adjoint process in $t \in \left[t_{s_2}, t_{s_3}\right]$ are multiplied by $i_{fd}(1+R_2)/R_w$ and $i_{fd}(1+R_2)/(R_wR_2)$ respectively, and are in-zoomed in Fig. 6. The optimal values for the switching times are $t_{s_1} = 0.8570$, $t_{s_2} = 1.4610$, $t_{s_3} = 1.5668$ which correspond to the switching states $x\left(t_{s_1}-\right) = 6\ \frac{\mathrm{m}}{\mathrm{s}} = 21.6\ \frac{\mathrm{km}}{\mathrm{h}}$, $x\left(t_{s_2}-\right) = 11.3897\ \frac{\mathrm{m}}{\mathrm{s}} = 41.0\ \frac{\mathrm{km}}{\mathrm{h}}$, $x\left(t_{s_3}-\right) = 10.6733\ \frac{\mathrm{m}}{\mathrm{s}} = 38.4\ \frac{\mathrm{km}}{\mathrm{h}}$ and the terminal state at $t_f = 6.3$ is $x\left(t_f\right) = 27.9534\ \frac{\mathrm{m}}{\mathrm{s}} = 100.6\ \frac{\mathrm{km}}{\mathrm{h}}$ which is slightly higher than the required speed due to numerical approximations in the solution of the above boundary value differential equations.

8. Concluding remarks

The electric vehicle equipped with a dual-stage planetary transmission studied in Section 4 highlights some of the key features of the hybrid systems framework presented in Section 2 and Appendix A. In particular, the modelling of the powertrain requires the consideration of both autonomous and controlled state jumps, some of which are accompanied by changes in the dimension of the state space. Furthermore, the corresponding hybrid automaton diagram for the full system presented in Fig. 3 exhibits a lot of the permitted behaviour of the completely general automaton in the definition of hybrid systems in Section 2 and Appendix A. It should be remarked that there is a genuine restriction by the automaton imposed on discrete transitions expressed in (i.e. corresponding to) those in the state transition structure displayed in Fig. 3.

The deterministic hybrid systems formulation of the driveline presented here provides a powerful framework for the study of deterministic optimal control problems associated with the gear changing problem of electric vehicles, such as those studied in Sections 6 and 7. For stochastic optimal control problems associated with non-deterministic tasks such as driving in uncertain environments, e.g. on heavy traffic roads, a further generalized framework for stochastic hybrid systems must be considered. One of the principal challenges in doing so is the presence of strict conditions for the termination of gear transitions due to the stick–slip phenomenon in the braking mechanisms in the transmission. The effect of such hard constraints imposed by switching manifolds on diffusion-driven state trajectories is studied in [36] in which the necessary optimality conditions are established in the form of the Stochastic Hybrid Minimum Principle (SHMP).

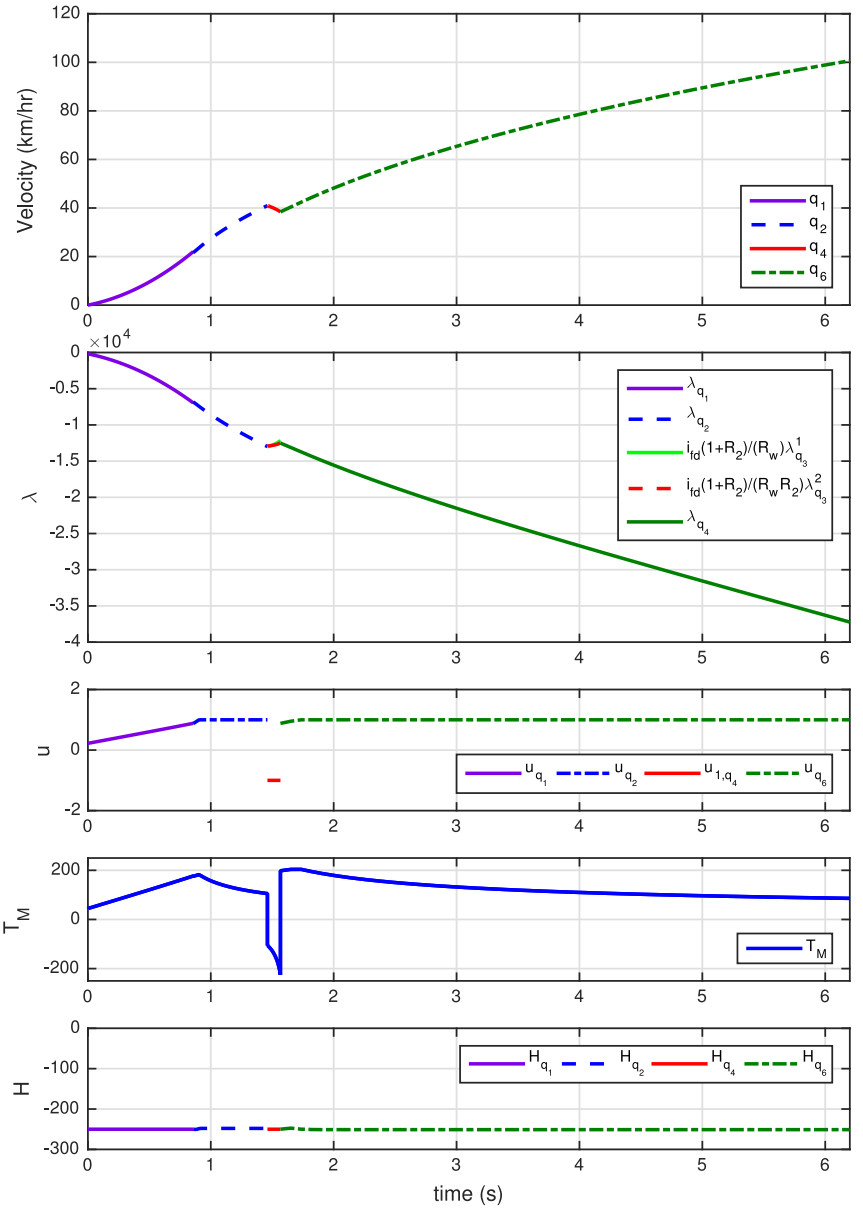

Fig. 5. The car speed, the adjoint processes and the corresponding Hamiltonians for the minimum energy acceleration task.

Acknowledgements

This work is supported by the Natural Sciences and Engineering Research Council of Canada (NSERC) (grant number: I228132C0G) and the Automotive Partnership Canada (APC) (grant number: I234504C0G). The authors would like to acknowledge the transmission design team at McGill University, and the industrial partners TM4, Linamar, and Infolytica.

Appendix A. Technical specifications and hypotheses

A.1. Hybrid systems

A *hybrid system (structure)* $\mathbb{H}$ is a septuple

$$\mathbb{H} = \{H := Q \times M, I := \Sigma \times U, \Gamma, A, F, \Xi, \mathcal{M}\}, \tag{A.1}$$

where the symbols in the expression and their governing assumptions are defined as below.

A0: $H := Q \times M$ is called the *(hybrid) state space* of the hybrid system $\mathbb{H}$, where

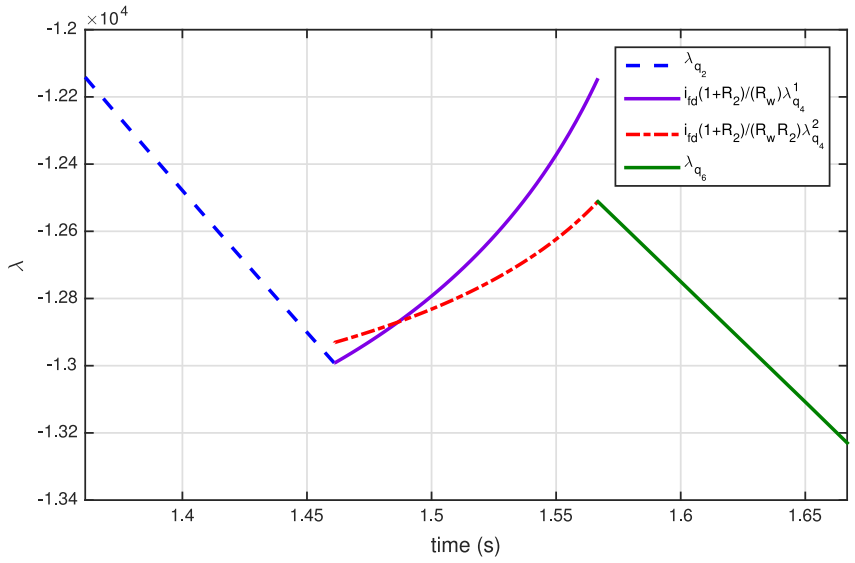

Fig. 6. Adjoint processes in the vicinity of the shifting process.

$Q = \{1, 2, \ldots, |Q|\} \equiv \left\{q_1, q_2, \ldots, q_{|Q|}\right\}$, $|Q| < \infty$, is a finite set of *discrete states (components)*, and
$M = \{\mathbb{R}^{n_q}\}_{q\in Q}$ is a family of finite dimensional continuous valued state spaces, where $n_q \leq n < \infty$ for all $q \in Q$.
$I := \Sigma \times U$ is the set of system input values, where
Σ with $|\Sigma| < \infty$ is the set of discrete state transition and continuous state jump events extended with the identity element, and
$U = \left\{U_q\right\}_{q\in Q}$ is the set of *admissible input control values*, where each $U_q \subset \mathbb{R}^{m_q}$ is a compact set in $\mathbb{R}^{m_q}$.
The set of admissible (continuous) control inputs $\mathcal{U}(U) := L_\infty([t_0, T_*), U)$, is defined to be the set of all measurable functions that are bounded up to a set of measure zero on $[t_0, T_*)$, $T_* < \infty$. The boundedness property necessarily holds since admissible input functions take values in the compact set U.
$\Gamma : H \times \Sigma \to H$ is a time independent (partially defined) *discrete state transition map*.
$\Xi : H \times \Sigma \to H$ is a time independent (partially defined) *continuous state jump transition map*. All $\xi_\sigma \in \Xi$, $\xi_\sigma : \mathbb{R}^{n_q} \to \mathbb{R}^{n_p}$, $p \in A(q, \sigma)$ are assumed to be continuously differentiable in the continuous state $x \in \mathbb{R}^{n_q}$.
$A : Q \times \Sigma \to Q$ denotes both a deterministic finite automaton and the automaton's associated transition function on the state space Q and event set Σ, such that for a discrete state $q \in Q$ only the discrete controlled and uncontrolled transitions into the q-dependent subset $\{A(q, \sigma), \sigma \in \Sigma\} \subset Q$ occur under the projection of Γ on its Q components: $\Gamma : Q \times \mathbb{R}^n \times \Sigma \to H|_Q$. In other words, Γ can only make a discrete state transition in a hybrid state (q, x) if the automaton A can make the corresponding transition in q.
F is an indexed collection of *vector fields* $\left\{f_q\right\}_{q\in Q}$ such that $f_q \in C^{k_{f_q}}\left(\mathbb{R}^{n_q} \times U_q \to \mathbb{R}^{n_q}\right)$, $k_{f_q} \geq 1$, satisfies a joint uniform Lipschitz condition, i.e. there exists $L_f < \infty$ such that $\left\|f_q(x_1, u_1) - f_q(x_2, u_2)\right\| \leq L_f(\|x_1 - x_2\| + \|u_1 - u_2\|)$, for all $x, x_1, x_2 \in \mathbb{R}^{n_q}$, $u, u_1, u_2 \in U_q$, $q \in Q$.
$\mathcal{M} = \{m_\alpha : \alpha \in Q \times Q, \}$ denotes a collection of *switching manifolds* such that, for any ordered pair $\alpha \equiv (\alpha_1, \alpha_2) = (q, r)$, m_α is a smooth, i.e. C^∞, codimension k sub-manifold of $\mathbb{R}^{n_q}$, $k \in \left\{1, \ldots, n_q\right\}$, described locally by $m_\alpha = \left\{x : m^1_\alpha(x) = 0 \wedge \cdots \wedge m^k_\alpha(x) = 0\right\}$, and possibly with boundary ∂m_α. It is assumed that $m_\alpha \cap m_\beta = \emptyset$, whenever $\alpha_1 = \beta_1$ but $\alpha_2 \neq \beta_2$, for all $\alpha, \beta \in Q \times Q$. □
We note that the case where m_α is identified with its reverse ordered version $m_{\bar{\alpha}}$ giving $m_\alpha = m_{\bar{\alpha}}$ is not ruled out by this definition, even in the non-trivial case $m_{p,p}$ where $\alpha_1 = \alpha_2 = p$. The former case corresponds to the common situation where the switching of vector fields at the passage of the continuous trajectory in one direction through a switching manifold is reversed if a reverse passage is performed by the continuous trajectory, while the latter case corresponds to the standard example of the bouncing ball.
Switching manifolds will function in such a way that whenever a trajectory governed by the controlled vector field meets the switching manifold transversally there is an autonomous switching to another controlled vector field or there is a jump transition in the continuous state component, or both. A transversal arrival on a switching manifold $m_{q,r}$, at state x occurs whenever

$$\nabla m^i_{q,r}(x)^T f_q(x, u) \neq 0, \tag{A.2}$$

for $u \in U_q$, $q, r \in Q$, $1 \leq i \leq k$.
A1: The initial state $h_0 := (q_0, x(t_0)) \in H$ is such that $m_{q_0,q_j}(x_0) \neq 0$, for all $q_j \in Q$. □

A.2. Hybrid optimal control problems

A2: Let $\{l_q\}_{q\in Q}, l_q \in C^{n_l}\left(\mathbb{R}^{n_q}\times U_q \to \mathbb{R}_+\right), n_l \geq 1$, be a family of running cost functions; $\{c_\sigma\}_{\sigma\in\Sigma} \in C^{n_c}\left(\mathbb{R}^{n_q}\times \Sigma \to \mathbb{R}_+\right), n_c \geq 1$, be a family of switching cost functions; and $g \in C^{n_g}\left(\mathbb{R}^{n_{q_f}} \to \mathbb{R}_+\right), n_g \geq 1$, be a terminal cost function satisfying the following assumptions:

(i) There exists $K_l < \infty$ and $1 \leq \gamma_l < \infty$ such that $\left|l_q(x_1,u_1) - l_q(x_2,u_2)\right| \leq K_l\left(\|x_1-x_2\| + \|u_1-u_2\|\right)$, for all $x_1, x_2 \in \mathbb{R}^{n_q}, u_1, u_2 \in U_q, q \in Q$.
(ii) There exists $K_c < \infty$ and $1 \leq \gamma_c < \infty$ such that $|c_\sigma(x)| \leq K_c\left(1+\|x\|^{\gamma_c}\right), \sigma \in \Sigma, x \in \mathbb{R}^{n_q}, q \in Q$.
(iii) There exists $K_g < \infty$ and $1 \leq \gamma_g < \infty$ such that $|g(x)| \leq K_g\left(1+\|x\|^{\gamma_g}\right), x \in \mathbb{R}^{n_{q_f}}, q_f \in Q$. □

Consider the initial time t_0, final time $t_f < \infty$, and initial hybrid state $h_0 = (q_0, x_0)$. For a fixed number of switchings $L < \infty$, let $\tau_L := \{t_0, t_1, t_2, \ldots, t_L\}$ be a strictly increasing sequence of times and $\sigma_i \in \Sigma, i \in \{1,2,\ldots,L\}$ extended with $\sigma_0 = id$ be a *discrete event sequence* that form a hybrid switching sequence

$$S_L = \left\{(t_0, id), \left(t_1, \sigma_{q_0q_1}\right), \ldots, \left(t_L, \sigma_{q_{L-1}q_L}\right)\right\} \equiv \left\{(t_0,q_0), (t_1,q_1), \ldots, (t_L,q_L)\right\}.$$

With the set of admissible continuous control inputs given as $\mathcal{U} = \bigcup_{i=0}^{L} L_\infty\left([t_i, t_{i+1}), U_{q_i}\right)$ with $t_{L+1} = t_f$, let $I_L := (S_L, u)$, $u \in \mathcal{U}$ be a finite *hybrid sequence of switching events* that results in a necessarily unique hybrid state process (see e.g. [7,28]).

Denote the set of all hybrid input trajectories with L switchings by $\boldsymbol{I_L}$. Then the Hybrid Optimal Control Problem (HOCP) is defined as the infimization of the hybrid cost (5) over the family of hybrid input trajectories $\boldsymbol{I_L}$, i.e.

$$J^o\left(t_0, t_f, h_0, L\right) = \inf_{I_L \in \boldsymbol{I_L}} J\left(t_0, t_f, h_0, L; I_L\right), \tag{A.3}$$

subject to (1)–(3) and possibly a number of switching manifold conditions as in (4). □

Appendix B. Euler–Lagrange derivation of the driveline dynamics

B.1. Powertrain dynamics in the fixed gear configuration

For the first gear ($\omega_R = 0$), the expression (30) for the kinetic energy T can be written in terms of the generalized coordinate $q = z$ using the kinematic relations (21)–(25), giving T as

$$T = \left(m + \frac{J_W}{r_W^2} + \left(\frac{J_M}{(R_1+1)^2} + J_S + \frac{J_{P,in}}{(R_1-1)^2} + \frac{J_{P,out}}{(R_2-1)^2}\right)\frac{i_{fd}^2(R_2+1)^2}{r_W^2}\right)\frac{v^2}{2}. \tag{B.1}$$

The virtual work (32) is given by the variational equation:

$$\delta W = \left(\frac{i_{fd}(R_2+1)}{r_W(R_1+1)}T_M - \frac{i_{fd}(R_2+1)}{r_W}T_{Sf} - \frac{i_{fd}^2(R_2+1)^2}{r_W^2}C_S v - \frac{1}{2}\rho C_d A_f v^2 - mgC_r\cos\gamma(z)\right)\delta z, \tag{B.2}$$

where for simplicity of the notation the sign function is removed assuming that the car is only moving forward, i.e. $v \geq 0 \Rightarrow \omega_S, \omega_R \geq 0$.

Forming the Lagrangian from (B.1) and (31) and substitution in the generalized Euler–Lagrange equation (29) with the generalized force determined from (B.2), the dynamics in the first gear is given as

$$\begin{aligned} &m\left(1 + \frac{J_W}{mr_W^2} + \left(\frac{J_M}{(R_1+1)^2} + J_S + \frac{J_{P,in}}{(R_1-1)^2} + \frac{J_{P,out}}{(R_2-1)^2}\right)\frac{i_{fd}^2(R_2+1)^2}{mr_W^2}\right)\dot{v} + mg\sin\gamma(z) \\ &= \frac{i_{fd}(R_2+1)}{r_W(R_1+1)}T_M - \frac{i_{fd}(R_2+1)}{r_W}T_{Sf} - \frac{i_{fd}^2(R_2+1)^2}{r_W^2}C_S v - \frac{1}{2}\rho C_d A_f v^2 - mgC_r\cos\gamma(z). \end{aligned} \tag{B.3}$$

Similarly, the dynamics in the second gear ($\omega_S = 0$) is found to be

$$\begin{aligned} &m\left(1 + \frac{J_W}{mr_W^2} + \left(\frac{R_1^2J_M}{(R_1+1)^2} + J_R + \frac{R_1^2J_{P,in}}{(R_1-1)^2} + \frac{R_2^2J_{P,out}}{(R_2-1)^2}\right)\frac{i_{fd}^2(R_2+1)^2}{mr_W^2R_2^2}\right)\dot{v} - mg\sin\gamma(z) \\ &= \frac{i_{fd}(R_2+1)R_1}{r_W(R_1+1)R_2}T_M - \frac{i_{fd}(R_2+1)}{r_WR_2}T_{Rf} - \frac{i_{fd}^2(R_2+1)^2}{r_W^2R_2^2}C_R v - \frac{1}{2}\rho C_d A_f v^2 - mgC_r\cos\gamma(z). \end{aligned} \tag{B.4}$$

B.2. Powertrain dynamics in the general configuration

Using the kinematic relations (21)–(25), the expression for T in terms of the generalized coordinate $q = [\theta_S, \theta_R]^T$ and its time differential $\dot{q} = [\omega_S, \omega_R]^T$ is written as

$$\begin{aligned} T &= \frac{1}{2} m \frac{r_W^2 \left(\omega_S + R_2 \omega_R\right)^2}{i_{fd}^2 \left(R_2+1\right)^2} + J_W \frac{\left(\omega_S + R_2 \omega_R\right)^2}{i_{fd}^2 \left(R_2+1\right)^2} + \frac{1}{2} J_M \frac{\left(\omega_S + R_1 \omega_R\right)^2}{\left(R_1+1\right)^2} \\ &\quad + \frac{1}{2} J_S \omega_S^2 + \frac{1}{2} J_R \omega_R^2 + \frac{1}{2} J_{P,in} \frac{\left(R_1 \omega_R - \omega_S\right)^2}{\left(R_1-1\right)^2} + \frac{1}{2} J_{P,out} \frac{\left(R_2 \omega_R - \omega_S\right)^2}{\left(R_2-1\right)^2}, \end{aligned} \tag{B.5}$$

or

$$\begin{aligned} T &= \frac{1}{2} \left(\frac{m r_W^2 + J_W}{i_{fd}^2 \left(R_2+1\right)^2} + \frac{J_M}{\left(R_1+1\right)^2} + J_S + \frac{J_{P,in}}{\left(R_1-1\right)^2} + \frac{J_{P,out}}{\left(R_2-1\right)^2} \right) \omega_S^2 \\ &\quad + \frac{1}{2} \left(\frac{\left(m r_W^2 + J_W\right) R_2^2}{i_{fd}^2 \left(R_2+1\right)^2} + \frac{J_M R_1^2}{\left(R_1+1\right)^2} + J_R + \frac{J_{P,in} R_1^2}{\left(R_1-1\right)^2} + \frac{J_{P,out} R_2^2}{\left(R_2-1\right)^2} \right) \omega_R^2 \\ &\quad + \left(\frac{\left(m r_W^2 + J_W\right) R_2}{i_{fd}^2 \left(R_2+1\right)^2} + \frac{J_M R_1}{\left(R_1+1\right)^2} - \frac{J_{P,in} R_1}{\left(R_1-1\right)^2} - \frac{J_{P,out} R_2}{\left(R_2-1\right)^2} \right) \omega_S \omega_R \\ &:= \frac{1}{2} J_{SS}\, \omega_S^2 + \frac{1}{2} J_{RR}\, \omega_R^2 + J_{SR}\, \omega_S\, \omega_R. \end{aligned} \tag{B.6}$$

In order to find D_i from (32), we rewrite the variational argument for the virtual displacements $\delta\theta_M$ and δz in terms of the generalized coordinates virtual displacements $\delta\theta_S$ and $\delta\theta_R$ using (21) and (23) to get

$$\delta W = \left(\frac{1}{R_1+1} T_M + T_{BS} + F_S + \frac{r_W}{i_{fd}\left(R_2+1\right)} F_r \right) \delta\theta_S + \left(\frac{R_1}{R_1+1} T_M + T_{BR} + F_R + \frac{r_W R_2}{i_{fd}\left(R_2+1\right)} F_r \right) \delta\theta_R. \tag{B.7}$$

Hence,

$$D_1 = \frac{1}{R_1+1} T_M + T_{BS} + F_S + \frac{r_W}{i_{fd}\left(R_2+1\right)} F_r, \tag{B.8}$$

$$D_2 = \frac{R_1}{R_1+1} T_M + T_{BR} + F_R + \frac{r_W R_2}{i_{fd}\left(R_2+1\right)} F_r, \tag{B.9}$$

since $q_1 = \theta_S$ and $q_2 = \theta_R$ are the selected generalized coordinates.

Forming the Lagrangian $L = T - V$ using (B.6) and (31), and substituting the generalized dissipative and driving forces from (B.7) in the Euler–Lagrange equation (29), the governing dynamics are derived as

$$J_{SS}\, \dot{\omega}_S + J_{SR}\, \dot{\omega}_R = D_1 + mg \sin\gamma\,(z)\, \frac{r_W}{i_{fd}\left(R_2+1\right)}, \tag{B.10}$$

$$J_{SR}\, \dot{\omega}_S + J_{RR}\, \dot{\omega}_R = D_2 + mg \sin\gamma\,(z)\, \frac{r_W R_2}{i_{fd}\left(R_2+1\right)}, \tag{B.11}$$

where to obtain (B.10) and (B.11), the relations

$$\frac{\partial L}{\partial \theta_S} = \frac{\partial L}{\partial z}\frac{\partial z}{\partial \theta_S} = \frac{-\partial V}{\partial z}\frac{\partial z}{\partial \theta_S} = -mg \sin\gamma\,(z)\, \frac{r_W}{i_{fd}\left(R_2+1\right)}, \tag{B.12}$$

$$\frac{\partial L}{\partial \theta_R} = \frac{\partial L}{\partial z}\frac{\partial z}{\partial \theta_R} = \frac{-\partial V}{\partial z}\frac{\partial z}{\partial \theta_R} = -mg \sin\gamma\,(z)\, \frac{r_W R_2}{i_{fd}\left(R_2+1\right)}, \tag{B.13}$$

have been used. Therefore,

$$\dot{\omega}_S = \frac{J_{RR}\left(D_1 + mg \sin\gamma\,(z)\, \frac{r_W}{i_{fd}(R_2+1)}\right)}{J_{SS}J_{RR} - J_{SR}^2} - \frac{J_{SR}\left(D_2 + mg \sin\gamma\,(z)\, \frac{r_W R_2}{i_{fd}(R_2+1)}\right)}{J_{SS}J_{RR} - J_{SR}^2}, \tag{B.14}$$

$$\dot{\omega}_R = \frac{J_{SS}\left(D_2 + mg \sin\gamma\,(z)\, \frac{r_W R_2}{i_{fd}(R_2+1)}\right)}{J_{SS}J_{RR} - J_{SR}^2} - \frac{J_{SR}\left(D_1 + mg \sin\gamma\,(z)\, \frac{r_W}{i_{fd}(R_2+1)}\right)}{J_{SS}J_{RR} - J_{SR}^2}. \tag{B.15}$$

Substituting D_1 and D_2 from (B.7) and assuming $\sin\gamma(z) \approx 0$ for the simplicity of the analysis, the dynamics of the powertrain is described by

$$\dot{\omega}_S = -A_{SS}\omega_S + A_{SR}\omega_R - A_{SA}(\omega_S + R_2\omega_R)^2 + B_{SS}T_{BS} - B_{SR}T_{BR} + B_{SM}T_M - D_{SL}, \tag{B.16}$$

$$\dot{\omega}_R = A_{RS}\omega_S - A_{RR}\omega_R - A_{RA}(\omega_S + R_2\omega_R)^2 - B_{RS}T_{BS} - B_{RR}T_{BR} + B_{RM}T_M - D_{RL}, \tag{B.17}$$

where

$$\begin{aligned}
A_{SS} &= \frac{J_{RR}C_S}{J_{SS}J_{RR} - J_{SR}^2}, \qquad A_{SR} = \frac{J_{SR}C_R}{J_{SS}J_{RR} - J_{SR}^2}, \qquad A_{SA} = \frac{\rho C_d A_f (J_{RR} - R_2 J_{SR}) r_W^3}{2\left(J_{SS}J_{RR} - J_{SR}^2\right) i_{fd}^3 (R_2+1)^3}, \\
B_{SS} &= \frac{J_{RR}}{J_{SS}J_{RR} - J_{SR}^2}, \qquad B_{SR} = \frac{J_{SR}}{J_{SS}J_{RR} - J_{SR}^2}, \qquad B_{SM} = \frac{J_{RR} - R_1 J_{SR}}{J_{SS}J_{RR} - J_{SR}^2}, \\
D_{SL} &= \frac{(J_{RR} - R_2 J_{SR}) r_W mgC_r}{i_{fd}(R_2+1)\left(J_{SS}J_{RR} - J_{SR}^2\right)} + \frac{J_{SR}T_{Rf} - J_{RR}T_{Sf}}{J_{SS}J_{RR} - J_{SR}^2},
\end{aligned} \tag{B.18}$$

and

$$\begin{aligned}
A_{RS} &= \frac{J_{SR}C_S}{J_{SS}J_{RR} - J_{SR}^2}, \qquad A_{RR} = \frac{J_{SS}C_R}{J_{SS}J_{RR} - J_{SR}^2}, \qquad A_{RA} = \frac{\rho C_d A_f (R_2 J_{SS} - J_{SR}) r_W^3}{2\left(J_{SS}J_{RR} - J_{SR}^2\right) i_{fd}^3 (R_2+1)^3}, \\
B_{RS} &= \frac{J_{SR}}{J_{SS}J_{RR} - J_{SR}^2}, \qquad B_{RR} = \frac{J_{SS}}{J_{SS}J_{RR} - J_{SR}^2}, \qquad B_{RM} = \frac{R_1 J_{SS} - J_{SR}}{J_{SS}J_{RR} - J_{SR}^2}, \\
D_{RL} &= \frac{(R_2 J_{SS} - J_{SR}) r_W mgC_r}{i_{fd}(R_2+1)\left(J_{SS}J_{RR} - J_{SR}^2\right)} + \frac{J_{SR}T_{Sf} - J_{SS}T_{Rf}}{J_{SS}J_{RR} - J_{SR}^2}.
\end{aligned} \tag{B.19}$$

We note that the brake torques T_{BS}, T_{BR} can only be resisting, i.e. $T_{BS} \in \left[-|T_{BS}|^{\max}, 0\right]$ and $T_{BR} \in \left[-|T_{BR}|^{\max}, 0\right]$.

References

[1] L. Pontryagin, V. Boltyanskii, R. Gamkrelidze, E. Mishchenko, The Mathematical Theory of Optimal Processes, Vol. 4, Wiley Interscience, New York, 1962.
[2] F.H. Clarke, R.B. Vinter, Optimal multiprocesses, SIAM J. Control Optim. 27 (5) (1989) 1072–1091.
[3] F.H. Clarke, R.B. Vinter, Applications of optimal multiprocesses, SIAM J. Control Optim. 27 (5) (1989) 1048–1071.
[4] H.J. Sussmann, Maximum principle for hybrid optimal control problems, in: Proceedings of the 38th IEEE Conference on Decision and Control, CDC, 1999, pp. 425–430.
[5] H.J. Sussmann, A Nonsmooth Hybrid Maximum Principle, in: Lecture Notes in Control and Information Sciences, vol. 246, Springer, London, 1999, pp. 325–354.
[6] X. Xu, P.J. Antsaklis, Optimal control of switched systems based on parameterization of the switching instants, IEEE Trans. Automat. Control 49 (1) (2004) 2–16.
[7] M.S. Shaikh, P.E. Caines, On the hybrid optimal control problem: Theory and algorithms, IEEE Trans. Automat. Control 52 (9) (2007) 1587–1603. corrigendum: 54, no. 6, (2009) 1428.
[8] F. Taringoo, P.E. Caines, On the optimal control of impulsive hybrid systems on Riemannian manifolds, SIAM J. Control Optim. 51 (4) (2013) 3127–3153.
[9] F. Taringoo, P. Caines, Gradient geodesic and Newton geodesic HMP algorithms for the optimization of hybrid systems, Annu. Rev. Control 35 (2) (2011) 187–198.
[10] M. Garavello, B. Piccoli, Hybrid necessary principle, SIAM J. Control Optim. 43 (5) (2005) 1867–1887.
[11] B. Passenberg, M. Leibold, O. Stursberg, M. Buss, The minimum principle for time-varying hybrid systems with state switching and jumps, in: Proceedings of the 50th IEEE Conference on Decision and Control and European Control Conference, CDC-ECC, 2011, pp. 6723–6729.
[12] A. Pakniyat, P.E. Caines, The hybrid minimum principle in the presence of switching costs, in: Proceedings of the 52nd IEEE Conference on Decision and Control, CDC, 2013, pp. 3831–3836.
[13] A. Pakniyat, P.E. Caines, On the relation between the minimum principle and dynamic programming for hybrid systems, in: Proceedings of the 53rd IEEE Conference on Decision and Control, CDC, 2014, pp. 19–24.
[14] A. Pakniyat, P.E. Caines, On the relation between the minimum principle and dynamic programming for classical and hybrid control systems, IEEE Trans. Automat. Control (2016) (submitted for publication) arXiv:1609.03158.
[15] M.S. Shaikh, P.E. Caines, On Relationships between Weierstrass-Erdmannn corner condition, Snell's law and the hybrid minimum principle, in: Proceedings of International Bhurban Conference on Applied Sciences and Technology, IBCAST, 2007, pp. 117–122.
[16] M.S.R. Mousavi, A. Pakniyat, T. Wang, B. Boulet, Seamless dual brake transmission for electric vehicles: Design, control and experiment, Mech. Mach. Theory 94 (2015) 96–118.
[17] M.S. Rahimi Mousavi, A. Pakniyat, B. Boulet, Dynamic modeling and controller design for a seamless two-speed transmission for electric vehicles, in: Proceedings of the 2014 IEEE Conference on Control Applications, CCA, 2014, pp. 635–640.
[18] A. Pakniyat, P.E. Caines, The gear selection problem for electric vehicles: An optimal control formulation, in: Proceedings of the 13th International Conference on Control Automation Robotics & Vision, ICARCV, IEEE, 2014, pp. 1261–1266.
[19] A. Bensoussan, J.L. Menaldi, Hybrid control and dynamic programming, Dyn. Contin. Discrete Impuls. Syst. Ser. B Appl. Algorithms 3 (4) (1997) 395–442.
[20] S. Dharmatti, M. Ramaswamy, Hybrid control systems and viscosity solutions, SIAM J. Control Optim. 44 (4) (2005) 1259–1288.
[21] G. Barles, S. Dharmatti, M. Ramaswamy, Unbounded viscosity solutions of hybrid control systems, ESAIM Control Optim. Calc. Var. 16 (1) (2010) 176–193.
[22] M.S. Branicky, V.S. Borkar, S.K. Mitter, A unified framework for hybrid control: Model and optimal control theory, IEEE Trans. Automat. Control 43 (1) (1998) 31–45.
[23] J. Lygeros, On reachability and minimum cost optimal control, Automatica 40 (6) (2004) 917–927.
[24] B. Passenberg, P. Kock, O. Stursberg, Combined time and fuel optimal driving of trucks based on a hybrid model, in: European Control Conference, ECC, 2009, pp. 4955–4960.

[25] E.I. Verriest, Multi-mode multi-dimensional systems, in: Proceedings of the 17th International Symposium on Mathematical Theory of Networks and Systems, MTNS, 2006, pp. 24–28.
[26] T.R. Mehta, D. Yeung, E.I. Verriest, M.B. Egerstedt, Optimal control of a multi-dimensional, hybrid ice-skater model, in: Proceedings of the 26th IEEE American Control Conference, 2007, pp. 2787–2792.
[27] A. Pakniyat, P.E. Caines, Time optimal hybrid minimum principle and the gear changing problem for electric vehicles in: Proceedings of the 5th IFAC Conference on Analysis and Design of Hybrid Systems, Atlanta, GA, USA, 2015, pp. 187–192.
[28] A. Pakniyat, Optimal control of deterministic and stochastic hybrid systems: Theory and applications (Ph.D. thesis), Department of Electrical & Computer Engineering, McGill University, Montreal, Canada, 2016.
[29] W. Fleming, R. Rishel, Deterministic and Stochastic Optimal Control, Springer, New York, 1975.
[30] A.D. Lewis, The Maximum Principle of Pontryagin in Control and in Optimal Control, Handouts for the course taught at the Universitat Politcnica de Catalunya, Department of Mathematics and Statistics Queens University, 2006.
[31] D. Liberzon, Calculus of Variations and Optimal Control Theory: A Concise Introduction, Princeton University Press, 2011.
[32] J. José, E. Saletan, Classical Dynamics: A Contemporary Approach, Cambridge University Press, 1998.
[33] H. Goldstein, C.P. Poole, J.L. Safko, Classical Mechanics, third ed., Addison-Wesley, 2001.
[34] A. Sciarretta, G. De Nunzio, L. Ojeda, Optimal ecodriving control: Energy-efficient driving of road vehicles as an optimal control problem, IEEE Control Syst. Mag. 35 (5) (2015) 71–90.
[35] N. Petit, A. Sciarretta, Optimal drive of electric vehicles using an inversion-based trajectory generation approach, in: Bittanti Sergio, Angelo Cenedese et Sandro Zampieri, éditeurs: Proceedings of the 18th IFAC World Congress, IFAC11, 2011, pp. 14519–14526.
[36] A. Pakniyat, P.E. Caines, On the stochastic minimum principle for hybrid systems, in: Proceedings of the 55th IEEE Conference on Decision and Control, Las Vegas, USA, 2016, (in press).